Heterologous production of glycine betaine using Synechocystis sp. PCC 6803-based chassis lacking native compatible solutes

Eunice A. Ferreira
IBMC: Instituto de Biologia Molecular e Celular
Catarina C. Pacheco
IBMC: Instituto de Biologia Molecular e Celular
João Rodrigues
Uppsala Universitet
Filipe Pinto
IBMC: Instituto de Biologia Molecular e Celular
Pedro Lamosa
ITQB: Universidade Nova de Lisboa Instituto de Tecnologia Quimica e Biologica
David Fuente
UPV: Universitat Politecnica de Valencia
Javier Urchueguía
UPV: Universitat Politecnica de Valencia
Paula Tamagnini (pmtamagn@ibmc.up.pt)
IBMC: Instituto de Biologia Molecular e Celular https://orcid.org/0000-0003-4396-2122

Research

Keywords: Compatible solutes, cyanobacteria, glycine betaine, glucosylglycerol, glutamate, salt stress, sucrose, Synechocystis , synthetic biology

Posted Date: November 1st, 2021

DOI: https://doi.org/10.21203/rs.3.rs-1031622/v1

Version of Record: A version of this preprint was published at Frontiers in Bioengineering and Biotechnology on January 7th, 2022. See the published version at https://doi.org/10.3389/fbioe.2021.821075.

Heterologous production of glycine betaine using *Synechocystis* sp. PCC 6803-based chassis lacking native compatible solutes

Eunice A. Ferreira[1,2,3], Catarina C. Pacheco[1,2], João S. Rodrigues[1,2,4,a], Filipe Pinto[1,2], Pedro Lamosa[5], David Fuente[6], Javier Urchueguía[6], Paula Tamagnini[1,2,4,*]

[1]i3S – Instituto de Investigação e Inovação em Saúde, Universidade do Porto, 4200-135 Porto, Portugal; [2]IBMC – Instituto de Biologia Molecular e Celular, Universidade do Porto, 4200-135 Porto, Portugal; [3]ICBAS – Instituto de Ciências Biomédicas Abel Salazar, Universidade do Porto, 4050-313 Porto, Portugal; [4]Departamento de Biologia, Faculdade de Ciências, Universidade do Porto, 4169-007 Porto, Portugal; [5]Instituto de Tecnologia Química e Biológica António Xavier, ITQB NOVA, 2780-157 Oeiras, Portugal; [6]Instituto de Aplicaciones de las Tecnologías de la Información y de las Comunicaciones Avanzadas, Universitat Politècnica de València, 46022 València, Spain.

[*]Corresponding author: Rua Alfredo Allen, 208, 4200-135 Porto, Portugal. Tel: +351 220 408 800. E-mail address: pmtamagn@ibmc.up.pt

Present Address: [a]Department of Chemistry – Ångström, Uppsala University, SE-751 20 Uppsala, Sweden.

Abstract

Background: Among compatible solutes, glycine betaine has various applications in the fields of nutrition, pharmaceuticals and cosmetics. Currently, this compound can be extracted from sugar beet plants or obtained by chemical synthesis, resulting in low yields or high carbon footprint, respectively. Hence, in this work we aimed at exploring the production of glycine betaine using the unicellular cyanobacterium *Synechocystis* sp. PCC 6803 as a photoautotrophic chassis.

Results: *Synechocystis* mutants lacking the native compatible solutes sucrose or/and glucosylglycerol - Δ*sps*, Δ*ggpS* and Δ*sps*Δ*ggpS* - were generated and characterized. Under salt stress conditions, the growth was impaired and accumulation of glycogen decreased by ~50% whereas the production of compatible solutes and extracellular polymeric substances (capsular and released ones) increased with salinity. These mutants were used as chassis for the implementation of a synthetic device based on the metabolic pathway described for the halophilic cyanobacterium *Aphanothece halophytica* for the production of the compatible solute glycine betaine. Transcription of ORFs comprising the device was shown to be stable and insulated from *Synechocystis'* native regulatory network. The production of glycine betaine was successfully obtained in all chassis tested, and was shown to increase with salinity. The introduction of the glycine betaine synthetic device into the Δ*ggpS* background improved its growth and enabled survival under 5% NaCl, which was not observed in the absence of the device. The maximum glycine betaine production was 64.29 µmol/gDW (1.89 µmol/mg protein) that was reached in the Δ*ggpS* chassis grown under 3% NaCl.

Conclusions: Taking into consideration the heterologous production of glycine betaine by our *Synechocystis* Δ*ggpS* chassis under seawater-like salinity, and the identification of main key players involved in the carbon fluxes, this work paves the way for a feasible production of this/or other compatible solutes, using optimized *Synechocystis* chassis in a pilot-scale.

Keywords: Compatible solutes; cyanobacteria; glycine betaine; glucosylglycerol; glutamate; salt stress; sucrose; *Synechocystis*; synthetic biology.

Background

Microorganisms can cope with environmental stresses such as temperature, salinity or drought via the production of compatible solutes (CS) – low-molecular weight organic compounds highly soluble in water that can accumulate intracellularly up to molar concentrations, without interfering with the cell metabolism (1). CS belong to different chemical classes including sugars (e.g. sucrose, trehalose), polyols (e.g. glycerol, sorbitol), heterosides (e.g. glucosylglycerol, floridoside), and amino acids or their derivatives (e.g. proline, glutamate, glycine betaine, ectoine) (2). Glycine betaine (or *N,N,N*-trimethylglycine) is an ubiquitous solute that can be found in bacteria, plants and mammals, being mostly synthesized by the two-step oxidation of choline to betaine aldehyde and subsequently to glycine betaine (3-5). Later on, the synthesis of glycine betaine via a three-step methylation of glycine was described in extremely halophilic bacteria (6, 7). This biosynthetic pathway involves two *N*-methyltransferases: the glycine-sarcosine-*N*-methyltransferase (GSMT) that catalyzes the methylation of glycine and sarcosine, and the dimethylglycine-*N*-methyltransferase (DMT) that converts dimethylglycine to glycine betaine. This CS has a strong stabilizing effect on biomolecules, by maintaining their structure and function (8, 9), and thus conferring drought-, osmo- and thermo-protection to cells (10-13). Moreover, glycine betaine plays an important physiological role as methyl group donor with beneficial stress-mitigating effects in humans (14, 15), and up-regulating antioxidant defense systems in plants (16, 17). Due to these interesting properties, glycine betaine is a value-added compound with applications in human nutrition, animal feed, agriculture, pharmaceuticals and cosmetics (14, 15, 18-21). Most of the commercially available glycine betaine is extracted from sugar beets (*Beta vulgaris*) (22), resulting in relatively low yields and rendering this organic production an expensive process. Alternatively, glycine betaine can be produced by chemical synthesis, but this process, although cheaper, has a high environmental impact increasing the carbon footprint (23, 24). A more sustainable and cost-effective production is highly desirable, and thus cyanobacteria emerge as promising chassis for the production of compatible solutes and other products of interest. Their photoautotrophic metabolism enables the sequestration and conversion of atmospheric CO_2 into organic compounds using sunlight and water as energy and

electron sources, respectively (25, 26). Therefore, they are being increasingly studied to be used as solar-powered cell factories for many biotechnological applications including the production of e.g. alcohols, alkanes, hydrogen, sugars and terpenoids (27-31). Among cyanobacteria, the unicellular *Synechocystis* sp. PCC 6803 (hereafter *Synechocystis*) is the best studied strain, and the vast array of data generated over the past decades allowed the construction of genome-scale metabolic models to predict system's behavior (32-35). Moreover, various molecular and synthetic biology tools are now available for the genetic manipulation and engineering of this particular cyanobacterial strain (36-39). *Synechocystis* is a freshwater strain and thus moderately halotolerant, relying on the biosynthesis of the compatible solutes sucrose, glutamate and glucosylglycerol to maintain the osmotic pressure under stress conditions (1, 40).

In this study, *Synechocystis* knockout mutants in the biosynthetic pathways producing the main native compatible solutes sucrose or/and glucosylglycerol were generated to serve as chassis for the production of value-added compounds. The genome-scale metabolic model *i*Syn811 was used to simulate the production rates of different heterologous CS and the highest rate was predicted for glycine betaine. As a proof-of-concept, we explored the production of this compatible solute using our *Synechocystis*-based chassis. For this purpose, a synthetic device based on the biosynthetic gene cluster from the halophilic cyanobacterium *Aphanothece halophytica* was constructed and introduced in the different chassis. Besides showing the production of glycine betaine and validating the functionality of the synthetic device, the characterization of the strains contributes to a better understanding of the mechanisms used by the cells to maintain homeostasis and cope with different levels of salinity.

Results

Generation of *Synechocystis* mutants deficient in the synthesis of native compatible solutes (CS)

The sustainable production of heterologous compatible solutes using *Synechocystis* as a chassis was envisioned in this work. The starting step was the generation of mutants deficient in the production of one or both of the main native compatible solutes, sucrose or glucosylglycerol

(GG). For this purpose, the genes encoding the enzymes involved in the first step of sucrose or/and GG synthesis (*sps* and *ggpS*, respectively), were knockout by double homologous recombination generating the *Synechocystis* markerless mutants Δ*sps*, Δ*ggpS*, and Δ*sps*Δ*ggpS* (for details see *Materials*). The complete segregation of the mutants was confirmed by PCR and Southern blot (**Additional file 1: Fig. S1 and Fig. S2**).

Effect of NaCl on the growth of *Synechocystis* wild-type and the CS deficient mutants

The growth of the CS deficient mutants under different salinities was analyzed. *Synechocystis* WT and mutants Δ*sps*, Δ*ggpS* and Δ*sps*Δ*ggpS* were grown in standard BG11 medium or in BG11 supplemented with 3, 5, and 7% (wt/vol) NaCl, corresponding to 510 mM, 860 mM and 1200 mM, respectively. The growth was monitored by measuring the OD_{730} and chlorophyll *a* (chl *a*) content (**Fig. 1**). In the absence of NaCl, the three mutants exhibited growth similar to the WT (**Fig. 1A**), indicating that the synthesis of sucrose and/or GG is nonessential under standard growth conditions. Nonetheless, challenging the cells with 3% NaCl had clear detrimental effects, with a ~23% growth decrease observed for the WT and CS single mutants Δ*sps* and Δ*ggpS* (**Fig. 1B** and **Additional file 1: Table S1**). The inactivation of both pathways in the Δ*sps*Δ*ggpS* mutant led to total growth arrest accompanied by a decline in chl *a* content (**Fig. 1B**; purple lines and **Additional file 1: Table S1**). A more pronounced impact was observed by increasing NaCl to 5%. The Δ*ggpS* could not grow in these conditions, while for the WT and Δ*sps*, a severe growth impairment (~49%) was observed (**Fig. 1C** and **Additional file 1: Table S1**). The growth of the latter two strains was similar up to day 7 however, after this period, the growth of Δ*sps* slowed down and by day 16 there was a significant difference ($P \leq 0.0001$) compared with the WT. The chl *a* content confirmed these observations (**Fig. 1C**; red and blue lines). Further increase in the NaCl concentration to 7% (wt/vol) showed that none of the strains tested could withstand the stress imposed (**Fig. 1D** and **Additional file 1: Table S1**).

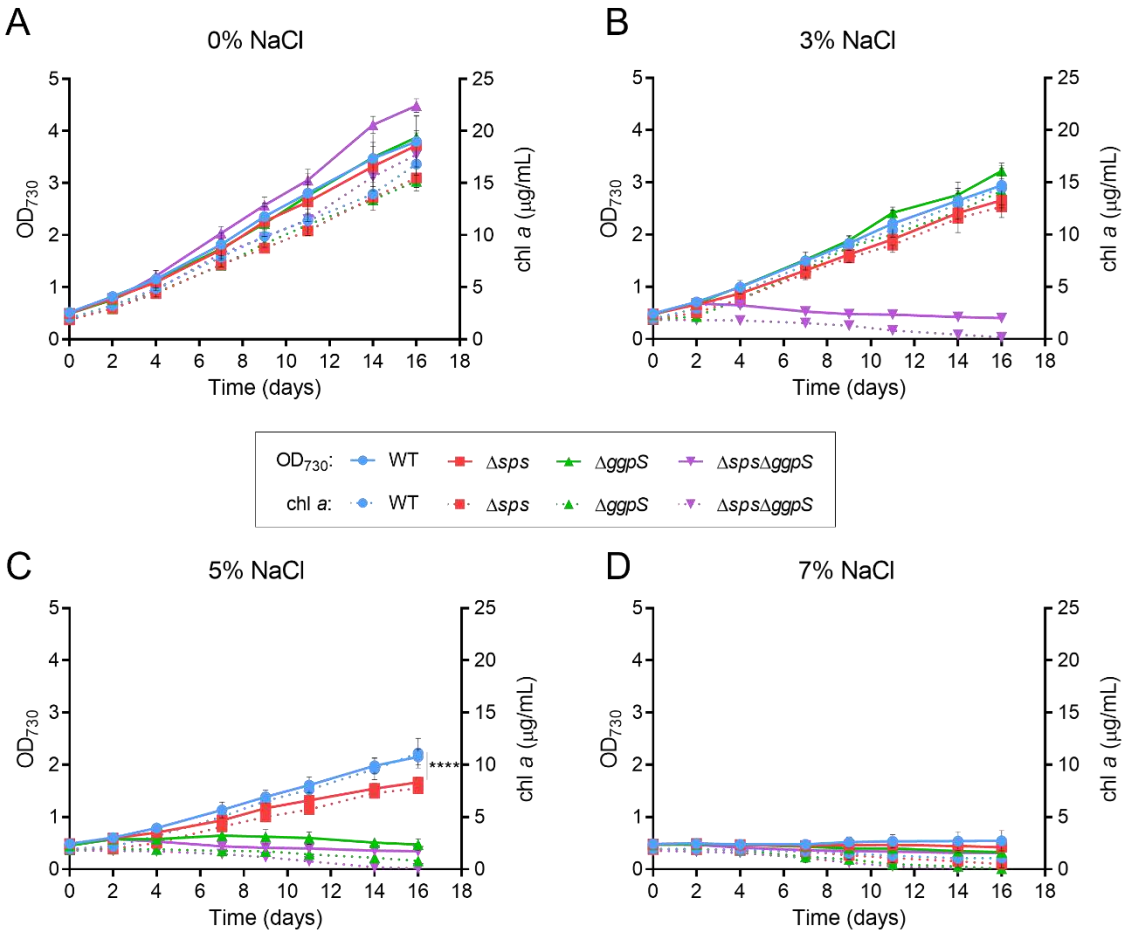

Fig. 1 - Growth curves of *Synechocystis* wild-type (WT) and Δ*sps*, Δ*ggpS* and Δ*sps*Δ*ggpS* mutants in BG11 (A) or BG11 supplemented with 3% (B), 5% (C) or 7% (D) (wt/vol) NaCl. Cultures were grown at 30 ºC with orbital shaking (150 rpm) under a 12 h light (25 µE/m^2/s) / 12 h dark regimen. Growth was monitored by measuring optical density at 730 nm (OD_{730}), and chlorophyll *a* (chl *a*) (full and dotted lines, respectively). Error bars correspond to standard deviations from at least three biological replicates with technical duplicates. Statistical analysis was performed using a two-way ANOVA, and a significant difference in terms of OD_{730} is identified by **** ($P \leq 0.0001$).

Quantification of CS in *Synechocystis* wild-type and the CS deficient mutants

The CS content was quantified in *Synechocystis* WT, Δ*sps*, Δ*ggpS* and Δ*sps*Δ*ggpS* mutants grown in BG11 or BG11 supplemented with NaCl (**Fig. 2**), under salinity conditions in which each strain could sustain growth (**Fig. 1**). In the WT, CS accumulation increased significantly in a salinity-dependent manner and GG was accumulated in higher amounts followed by glutamate and sucrose (**Fig. 2A**). As expected, the two main compatible solutes sucrose and GG could only be

detected in the presence of NaCl. The amino acid glutamate was detected in all backgrounds and conditions, and increased more than 1.8-fold in the presence of salinity (significant difference $P \leq 0.01$ for WT in 0% and 5% NaCl). In the Δ*sps*, Δ*ggpS* and Δ*sps*Δ*ggpS* mutants the absence of sucrose and/or GG production was confirmed (**Fig. 2B, 2C** and **2D**). For the Δ*sps*, a salinity-dependent accumulation of GG was also detected (**Fig. 2B**), however, the GG concentration was 50% lower compared with the WT, under 5% NaCl. In contrast, the Δ*ggpS* mutant accumulated 17-fold more sucrose than the WT, under 3% NaCl (**Fig. 2C**). All the proton NMR spectra are depicted in **Additional file 1: Fig. S3**.

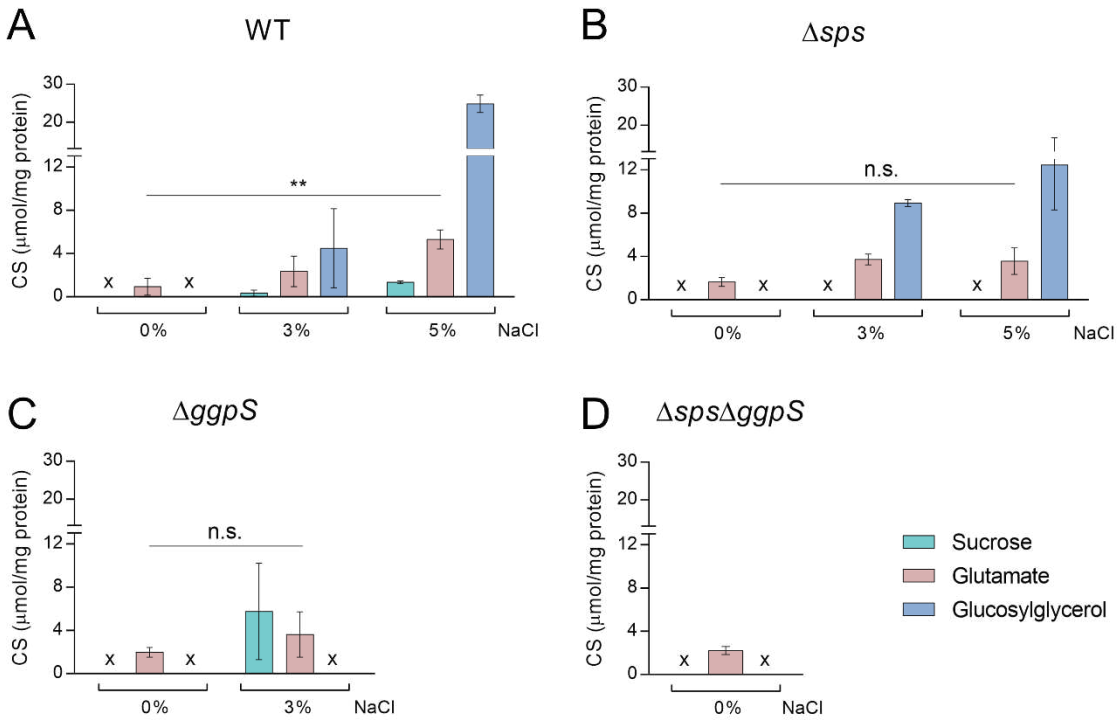

Fig. 2 - Effect of NaCl on the synthesis of native compatible solutes sucrose, glutamate and glucosylglycerol by *Synechocystis* wild-type (WT) (A), and the Δ*sps* (B), Δ*ggpS* (C) and Δ*sps*Δ*ggpS* mutants (D). Cultures were grown in BG11 or BG11 supplemented with 3% or 5% (wt/vol) NaCl, at 30 ºC with orbital shaking (150 rpm) under a 12 h light (25 µE/m^2/s) / 12 h dark regimen, and cells were harvested four days after inoculation (initial $OD_{730} \approx 0.5$). Compatible solutes were quantified by H-NMR and the results were normalized per mg of protein. x - not detected. Error bars correspond to standard deviations from at least three biological replicates. Statistical analysis was performed using two-way ANOVA. Statistically significant differences are identified: ** ($P \leq 0.01$) and n.s. (not significant).

Effect of NaCl on total carbohydrates, glycogen, capsular (CPS) and released (RPS) polysaccharides

In addition to the CS pools, the total carbohydrate content was analyzed in *Synechocystis* WT and the CS deficient mutants (**Fig. 3A**). Generally, the presence of salinity (3 or 5% NaCl) had no significant impact on the production of total carbohydrates, except for the Δ*sps* mutant that showed some fluctuation when exposed to different salinities (**Fig. 3A**; $P \leq 0.05$). To further clarify the carbon distribution in response to salinity, the amount of glycogen as well as the production of extracellular polymeric substances, CPS and RPS, were also determined (**Fig. 3B, 3C** and **3D**). The presence of NaCl led to a significant decrease in the amount of glycogen in the WT, Δ*sps* and Δ*ggpS*, with reductions of more than 56%, independent of the salinity concentration and the deletion of one of the CS pathways (**Fig. 3B**). In terms of capsular polysaccharides (CPS), the opposite effect was observed with a 2.4-fold increase in CPS for the WT and the Δ*sps* at 5%, and a 2.1-fold increase for Δ*ggpS* at 3% NaCl, compared with 0% NaCl (**Fig. 3C**). The amount of RPS produced by WT or Δ*ggpS* did not change significantly whereas for the Δ*sps* a 2.5-fold increase was registered under 5% NaCl (**Fig. 3D**). Staining the WT and Δ*sps* cultures with Alcian Blue confirmed similar RPS production for the WT under 0% and 5% NaCl, while for the Δ*sps* the accumulation of RPS in 5% NaCl is evident, leading to the formation of cell aggregates (**Fig. 3E**; black arrowhead).

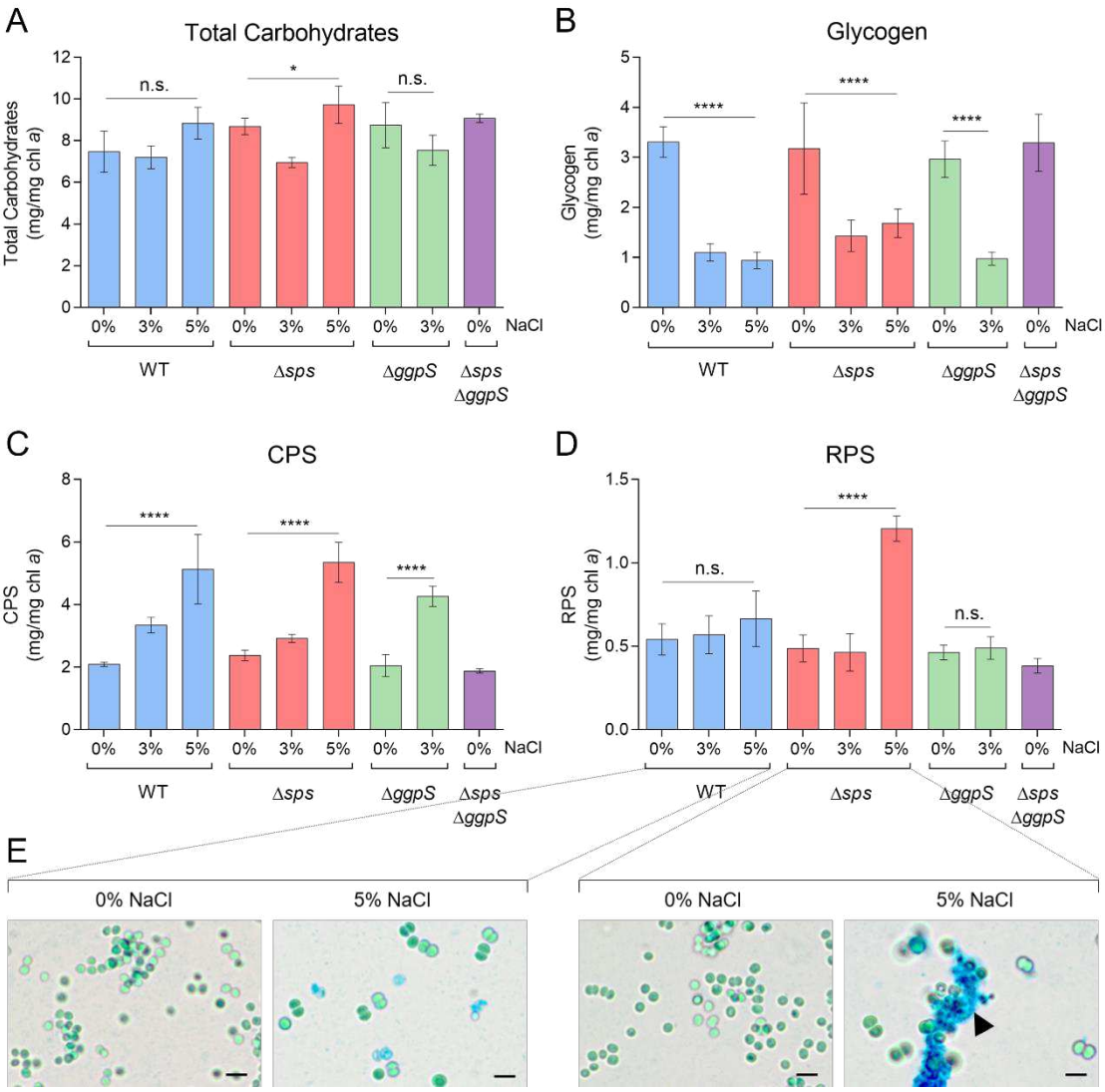

Fig. 3 - Effect of NaCl on total carbohydrates (A), glycogen (B), CPS - capsular polysaccharides (C) and RPS - released polysaccharides (D) produced by *Synechocystis* wild-type (WT) and the Δ*sps,* Δ*ggpS* and Δ*sps*Δ*ggpS* mutants. Cells were grown in BG11 or BG11 supplemented with 3% or 5% (wt/vol) NaCl, at 30 ºC with orbital shaking (150 rpm) under a 12 h light (25 µE/m^2/s) / 12 h dark regimen for 16 days. Results are expressed as milligrams per milligram of chlorophyll *a* (chl *a*). Error bars correspond to standard deviations from at least three biological replicates, with technical triplicates. Statistical analysis was performed using one-way ANOVA. Statistically significant differences are identified: **** ($P \leq 0.0001$), * ($P \leq 0.05$) and n.s. (not significant). Light micrographs **(E)** of *Synechocystis* WT and Δ*sps* cultures grown in BG11 or BG11 supplemented with 5% NaCl and stained with Alcian Blue; the black arrowhead highlights RPS production by the Δ*sps* mutant under 5% NaCl. Scale bars: 5 µm.

205 ***In silico*** **prediction of production rates for native and heterologous CS using** ***Synechocystis***
206 **wild-type**

207 The genome-scale metabolic model of *Synechocystis* – *i*Syn811 (33) – was updated to include all
208 the information required for calculating CS production rates. The manual curation process started
209 with the addition of the metabolic precursors and the reactions required for CS synthesis. The
210 nomenclature was also corrected and standardized, and the reversibility of some reactions was
211 changed (for more details see the *Materials* section). After the curation of the metabolic model
212 was completed, the COBRA ("The COnstraint-Based Reconstruction and Analysis") Toolbox
213 v3.0 (41), was used to simulate the compatible solute production rate as a function of
214 *Synechocystis* wild-type growth under autotrophic conditions (**Fig. 4**). The results show a linear
215 tradeoff between the cell's resources toward growth or the production of the different CS.
216 Regarding the production of the native CS, GG and sucrose impose a higher metabolic burden
217 showing lower *in silico* production rates (0.378 and 0.283 mmol/gDW/h, respectively), compared
218 with glutamate (0.567 mmol/gDW/h). The simulation of the production of heterologous CS
219 glycine betaine (GB) showed the best compromise between growth and production compared
220 with the three native CS, with the highest predicted maximum production rate of 0.680
221 mmol/gDW/h. In addition to GB, the production rates of other heterologous CS, such as ectoine
222 and mannosylglycerate were also simulated, revealing that the maximum production rate
223 predicted for these two solutes is lower than the obtained for GB (**Additional file 1: Fig. S4**).
224 Hence, GB was chosen as the heterologous CS to be produced using the *Synechocystis* chassis
225 developed (CS-deficient mutants).
226

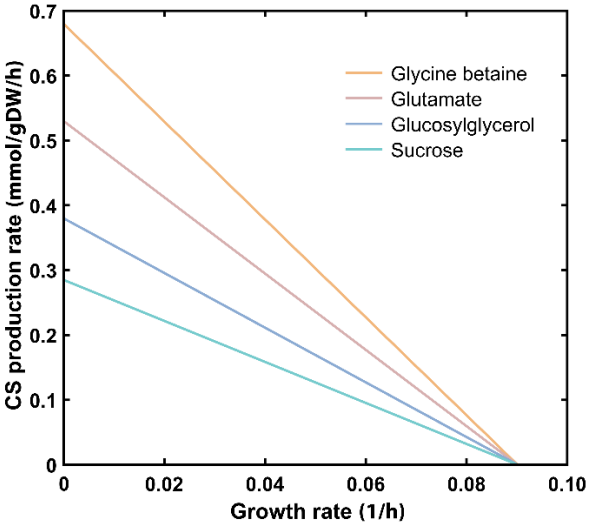

Fig. 4 - Theoretical productivity of the heterologous compatible solute glycine betaine and the native ones (glutamate, glucosylglycerol and sucrose), as predicted by the updated version of the genome-scale metabolic model *i*Syn811. The lines represent the compatible solute production rate as a function of *Synechocystis* wild-type growth under autotrophic conditions.

Design and assembly of the synthetic device for the production of glycine betaine (GB)

Envisaging the heterologous production of GB, a synthetic device was designed based on the metabolic pathway described for the halophilic cyanobacterium *Aphanothece halophytica* (**Fig. 5A**) (6, 7). This device comprises two Open Reading Frames (ORFs) encoding the enzymes involved in the three-step methylation of glycine to glycine betaine: glycine-sarcosine-*N*-methyltransferase (*gsmt*), and the dimethylglycine-*N*-methyltransferase (*dmt*). In these reactions, *S*-adenosylmethionine (SAM) is the source of methyl groups for the synthesis of GB, and it can be synthesized from L-methionine by the *S*-adenosyl-methionine synthase (MetX) (**Fig. 5A**). To prevent the shortage of the SAM precursor, the ORF encoding *Synechocystis'* native MetX (*metX*, *sll0927*) was also included in the device. The sequences of the three ORFs (*gsmt*, *dmt* and *metX*) were codon-optimized and restriction sites incompatible with the BioBrick standard RFC[10] were eliminated. Subsequently, the ribosome binding site (RBS) BBa_B0030 and double stop codons (TAATAA) were included before and after each ORF, respectively. A double terminator (BBa_B0015) was also included at the end of the synthetic construction (Ahbet). Additionally, the designed DNA sequence was flanked by the prefix and suffix of the BioBrick RFC[10]

standard (42), enabling the use of the standard assembly method to include the regulatory element (promoter). After DNA synthesis, the Ahbet construction was cloned downstream of the promoter $P_{trc.x.lacO}$, originating the $P_{trc.x.lacO}$::Ahbet synthetic device (hereafter GB device) (**Fig. 5B**). The $P_{trc.x.lacO}$ is a constitutive promoter in *Synechocystis*, previously characterized by our group and is 41-fold stronger than the reference cyanobacterial promoter P_{rnpB} (43).

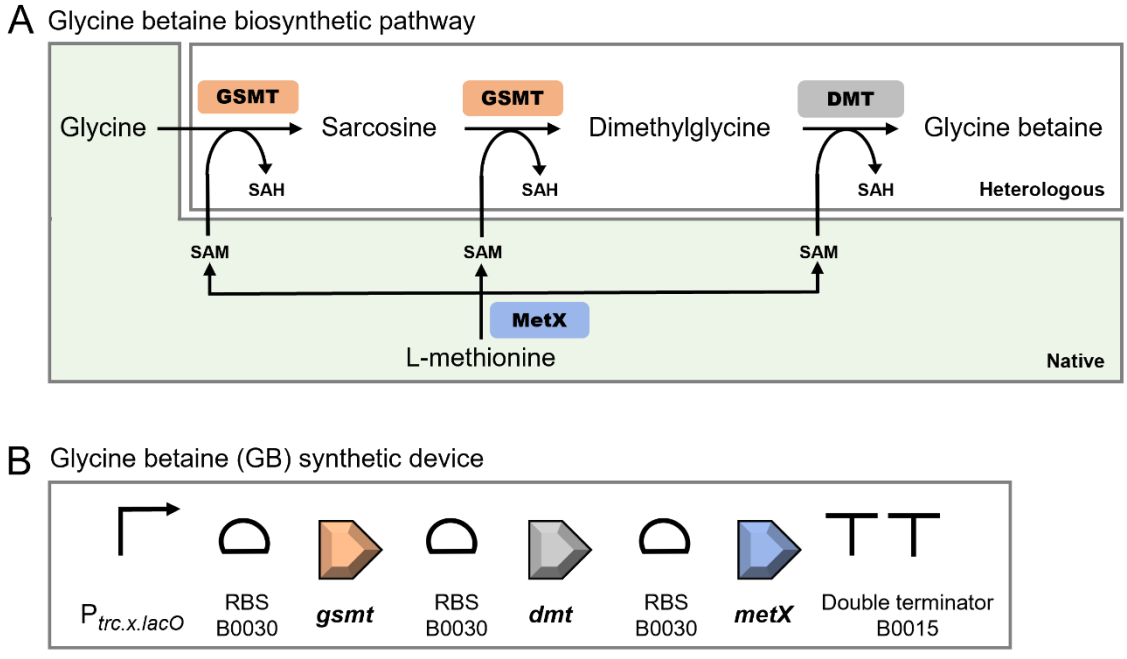

Fig. 5 - Glycine betaine biosynthetic pathway (A) and schematic representation of the glycine betaine (GB) synthetic device for the production of this heterologous compatible solute in *Synechocystis* (B). The glycine betaine biosynthetic pathway comprises the GSMT (glycine-sarcosine-*N*-methyltransferase) and DMT (dimethylglycine-*N*-methyltransferase) from *Aphanothece halophytica* (heterologous), and MetX (*S*-adenosyl-methionine synthase) from *Synechocystis* (native). SAM - *S*-adenosyl-methionine; SAH - *S*-adenosyl-homocysteine. The GB device includes the promoter $P_{trc.x.lacO}$, the ribosomal binding site (RBS) B0030, the open reading frames *gsmt*, *dmt* and *metX* codon optimized for *Synechocystis*, and the double terminator B0015.

Effect of the implementation of the GB device into the *Synechocystis* chassis

The GB synthetic device was implemented into the *Synechocystis* WT and the CS deficient Δ*ggpS* and Δ*sps*Δ*ggpS* chassis described above, using the replicative plasmid pSEVA351. The device was not introduced into Δ*sps* since the characterization showed that this mutant is similar to the

WT in terms of growth, total carbohydrates, glycogen content and CPS (**Fig. 1, Fig. 3A, Fig. 3B** and **Fig. 3C**, respectively). The presence of the GB device in the cells was confirmed by PCR (**Additional file 1: Fig. S5**), and the growth and chl *a* content of the transformants were monitored in absence/presence of salinity and compared with the respective backgrounds (**Fig. 6** and **Additional file 1: Fig. S6**). As shown in **Fig. 6**, the introduction of the synthetic device had distinct effects depending on the genetic background. The implementation of GB device into Δ*ggpS* led to a significant improvement of growth (16%) in BG11 and BG11 supplemented with 3% NaCl (**Fig. 6A** and **6B**; green lines), and supported its survival under 5% NaCl (**Fig. 6C**; green lines). After 16 days of cultivation under 5% NaCl, the batch culture of Δ*ggpS* showed clear signs of chlorosis/necrosis while the culture of the Δ*ggpS* mutant harboring the GB device remained green (**Fig. 6C**; insert). In agreement, the chl *a* content was 0.8 µg/mL and 1.8 µg/mL, respectively (**Additional file 1: Fig. S6**; green lines). Notably, this survival phenotype was observed for at least 25 days (data not shown). In the WT background the presence of the device had a detrimental effect on growth (~15% decrease) in all conditions tested (**Fig. 6**; blue lines). The growth of the double mutant Δ*sps*Δ*ggpS* in the absence of NaCl was not affected by the introduction of the synthetic device (**Fig. 6A**; purple lines). Moreover, the mutant harboring the GB device was unable to survive under saline conditions, similarly to what happened to Δ*sps*Δ*ggpS* background (**Fig. 6B, 6C,** and **6D**; purple lines).

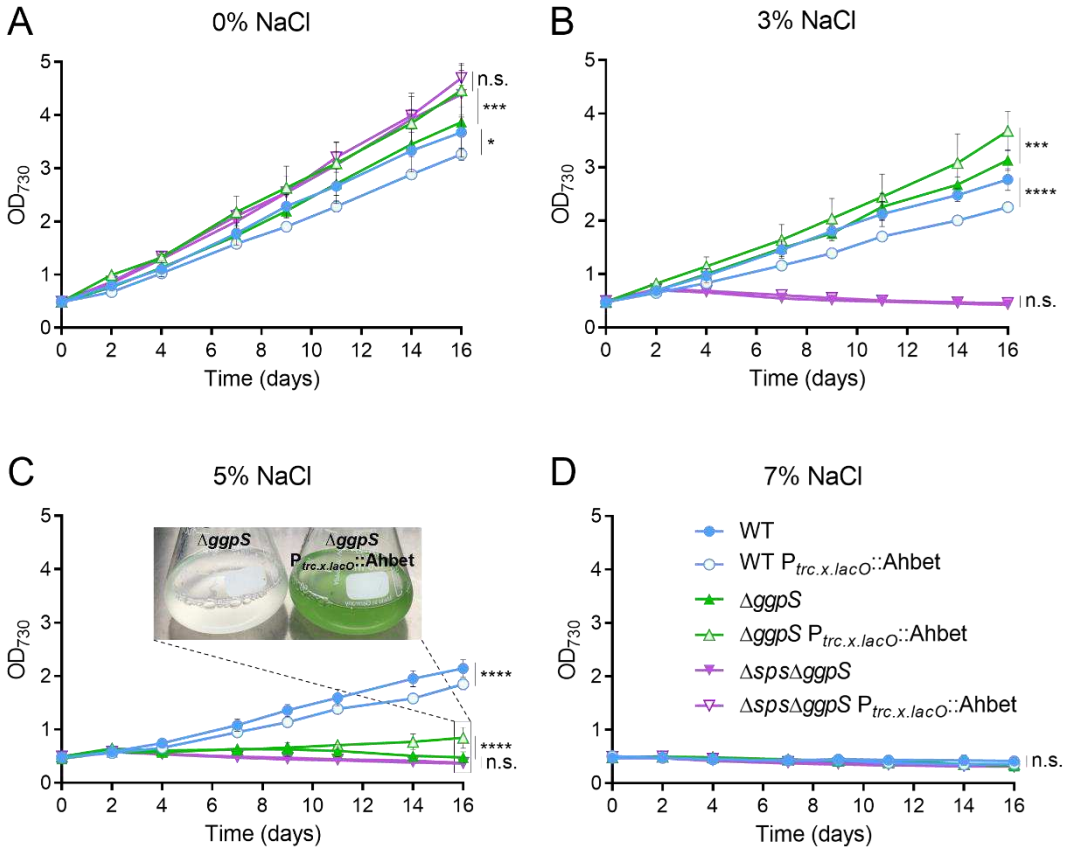

Fig. 6 - Growth of *Synechocystis* wild-type (WT), Δ*ggpS* and Δ*sps*Δ*ggpS* without or with the GB device ($P_{trc.x.lacO}$::Ahbet). Cultures were grown in BG11 (**A**) or BG11 supplemented with 3% (**B**), 5% (**C**) or 7% (**D**) (wt/vol) NaCl, at 30 ºC with orbital shaking (150 rpm) under a 12 h light (25 µE/m^2/s) / 12 h dark regimen. Growth was monitored by measuring the optical density at 730 nm (OD_{730}). Error bars correspond to standard deviations from at least three biological replicates with technical duplicates. Statistical analysis was performed using two-way ANOVA. Statistically significant differences are identified: **** ($P \leq 0.0001$), *** ($P \leq 0.001$), * ($P \leq 0.05$) and n.s. (not significant). In Fig. 6C, the liquid cultures of *Synechocystis* Δ*ggpS* (left) and Δ*ggpS* $P_{trc.x.lacO}$::Ahbet (right), in BG11 supplemented with 5% NaCl after 16 days of cultivation, are shown.

Analysis of transcript levels in *Synechocystis* strains harboring the GB device

The next step in the characterization of the different *Synechocystis* strains harboring the GB device was the evaluation of the transcript levels of the three ORFs comprised in the device (*gsmt*, *dmt* and *metX*) by RT-qPCR (for more details see the *Materials* section). As shown in **Fig. 7**, the transcripts of the three genes (*gsmt*, *dmt* and *metX*) were detected in all samples and the relative

304 expression was reasonably stable independently of the background strain. Additionally, the
305 relative expression remained similar under salinity conditions and, even though some variation
306 could be detected, it was not statistically significant (**Additional file 1: Table S2**).
307

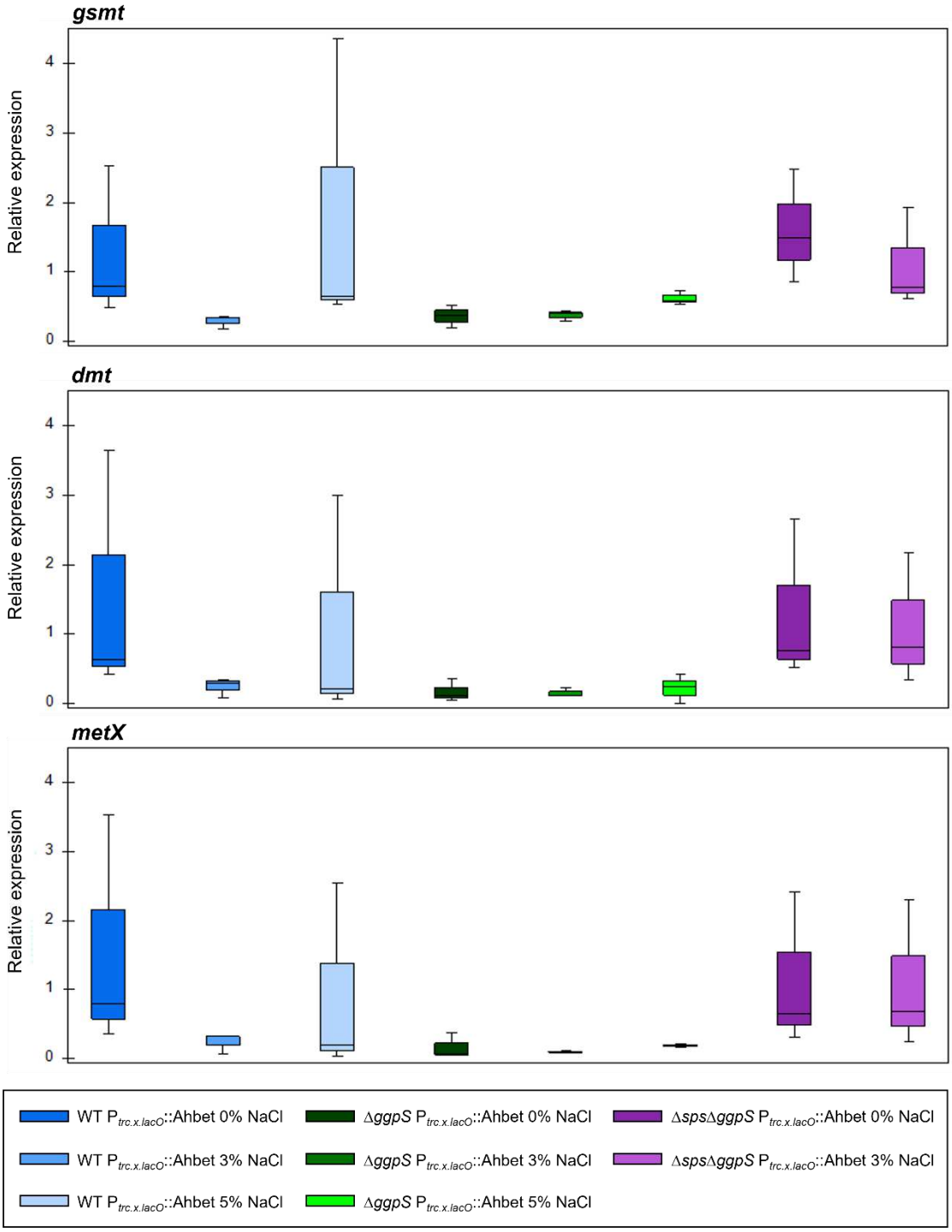

308

309 **Fig. 7 - RT-qPCR analysis of *gsmt*, *dmt* and *metX* relative expression in *Synechocystis* strains**
310 **(WT, Δ*ggpS* and Δ*sps*Δ*ggpS*) harboring the GB device**. RNA was extracted from cells grown

311 in BG11 or BG11 supplemented with 3% and 5% (wt/vol) NaCl, at 30 ºC with orbital shaking
312 (150 rpm) under a 12 h light (25 μE/m^2/s) / 12 h dark regimen. The box-whisker plots represent
313 the expression of the target genes relative to WT $P_{trc.x.LacO}$::Ahbet in absence of salt (0% NaCl).
314 Data were obtained from three biological replicates and three technical replicates, and the
315 whiskers represent the minimum and maximum non-outlier values in the dataset. One-way
316 ANOVA was performed no significant differences could be detected.
317

318 **Quantification of native and heterologous CS in *Synechocystis* chassis harboring the GB**
319 **device**

320 The CS pool of the different *Synechocystis* strains (WT, Δ*ggpS* and Δ*sps*Δ*ggpS*) harboring the
321 GB device was analyzed in absence/presence of NaCl after 4 days of cultivation (**Fig. 8**). The
322 results obtained confirmed that the implementation of the pathway for the synthesis of
323 heterologous CS was successful, since glycine betaine could be detected in all strains and
324 conditions analyzed. Under 0% and 3% NaCl, the presence of the GB device in the WT
325 background did not significantly influence the synthesis of native CS and heterologous production
326 of GB is not significantly influenced by salinity. However, under 5% NaCl, there was an impact
327 on the synthesis of glutamate and GG that decreased by 59% and 62%, respectively, and the
328 synthesis of GB increased 2.7-fold compared with 0% NaCl (**Fig. 8A** and **Fig. 2A**). Similarly, the
329 implementation of the device in the Δ*ggpS* did not affect the production of the native CS under
330 0% and 3% NaCl compared with Δ*ggpS* chassis (**Fig. 8B** and **Fig. 2C**). However, the introduction
331 of the device into the Δ*ggpS* background allowed this strain to survive under 5% NaCl and,
332 therefore the quantification of CS was also performed. The results obtained showed that in Δ*ggpS*
333 $P_{trc.x.lacO}$::Ahbet, besides glycine betaine production, the levels of sucrose and glutamate were
334 similar to the ones observed for 3% NaCl (**Fig. 8B**). An analysis of the Δ*ggpS* harboring the GB
335 device after 16 days of cultivation suggested that the production of all CS is maintained for at
336 least two weeks of cultivation (**Additional file 1: Fig. S7**). For the double mutant, the presence
337 of the device led to a significant decrease (71%) of glutamate in the absence of salinity (**Fig. 8C**
338 and **Fig. 2D**). In contrast, under 3% NaCl, there was a 2.5-fold increase in glutamate ($P \leq 0.0001$)
339 compared with 0% NaCl, while the glycine betaine content remained similar (**Fig. 8C**). All the

proton NMR spectra are depicted in **Additional file 1: Fig. S8**. Furthermore, the CS quantification was also performed for the extracellular medium, and the results showed that none of the native CS could be detected, while GB was detected in negligible amounts in all strains harboring the device and conditions tested (**Additional file 1: Table S3**).

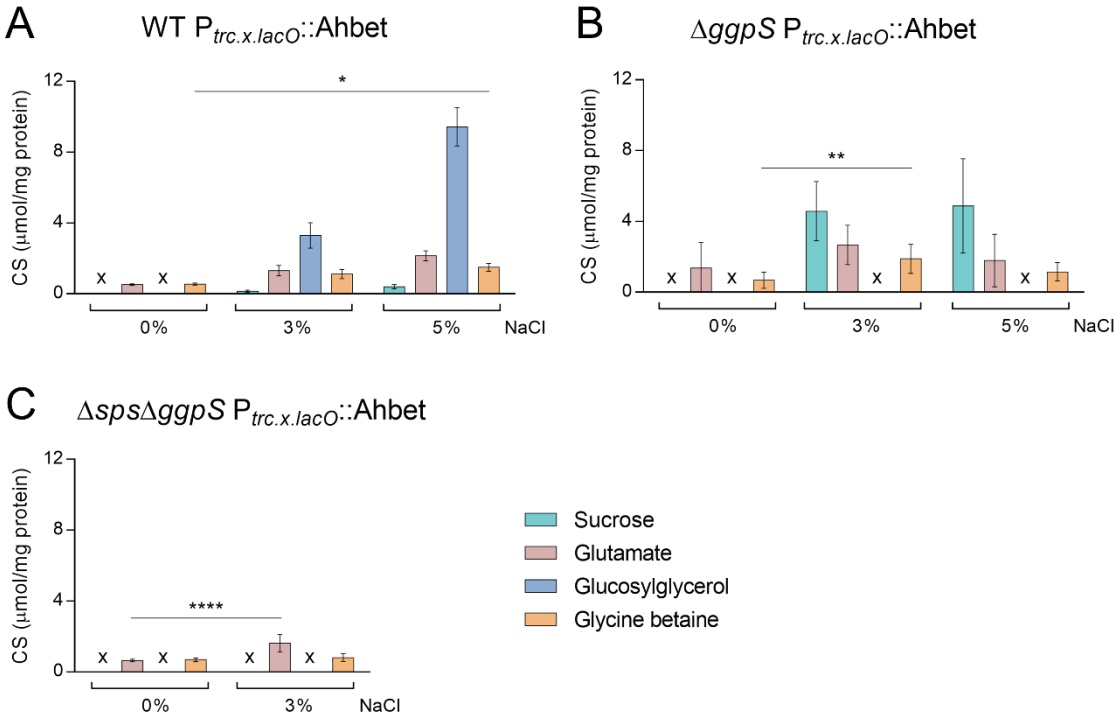

Fig. 8 – Production of glycine betaine (GB) and native compatible solutes in different *Synechocystis* strains harboring the GB device: WT (wild-type) $P_{trc.x.lacO}$::Ahbet (A), Δ*ggpS* $P_{trc.x.lacO}$::Ahbet (B), and Δ*sps*Δ*ggpS* $P_{trc.x.lacO}$::Ahbet (C). Cultures were grown in BG11 or BG11 supplemented with 3% or 5% (wt/vol) NaCl, at 30 ºC with orbital shaking (150 rpm) under a 12 h light (25 µE/m^2/s) / 12 h dark regimen; and cells were harvested four days after inoculation (initial $OD_{730} \approx 0.5$). Compatible solutes were quantified by H-NMR and the results were normalized per mg of protein. x - not detected. Error bars correspond to standard deviations from three biological replicates. Statistical analysis was performed using two-way ANOVA. Statistically significant differences are identified: **** ($P \leq 0.0001$), ** ($P \leq 0.01$) and * ($P \leq 0.05$).

Discussion

The sustainable production of compatible solutes (CS) is essential for pharmaceutical and cosmetic industries. The current microbiological processes have a significant negative impact on the environment, which could be mitigated by the use of photoautotrophic chassis such as cyanobacteria. For the synthesis of heterologous CS in *Synechocystis*, the construction of customized chassis is required and our strategy was to eliminate competing or redundant pathways. Therefore, in this work we have generated three *Synechocystis* mutants deficient in the production of native compatible solutes (namely, sucrose or/and glucosylglycerol). These strains – Δ*sps*, Δ*ggpS*, and Δ*sps*Δ*ggpS* – were characterized under different salinity concentrations, expanding the knowledge that will allow further optimization of the chassis for the increased production of heterologous CS, such as glycine betaine (GB). In this context, an updated version of the genome-scale metabolic model of *Synechocystis* – *i*Syn811 (33) – was used to predict the production rates for native and heterologous CS using *Synechocystis* wild-type. The simulations show a linear tradeoff between deviating resources toward cellular growth or toward the production of the solutes. Since energy and carbon uptake are limited, any extra need of ATP or carbon molecules for compatible solute synthesis will impair cell growth. Whether carbon or light uptake is limiting the synthesis of each CS is difficult to predict, since alternative routes with different energetic efficiencies can be simultaneously active under different growth conditions. From the CS evaluated, the predictions indicate that the synthesis of native sucrose and glucosylglycerol (GG) has a higher impact on cell growth than glutamate or the heterologous solute glycine betaine (GB) (**Fig. 4**). The production of sucrose and GG require glucose that drains more cell resources than the reported for the synthesis of an amino acid (44), such as glutamate or glycine (the latter required for GB production). The results also suggest that the production of GB has a smaller restraining effect on growth than glutamate or other heterologous CS, like ectoine and mannosylglycerate (**Additional file 1: Fig. S4**).

In parallel, the evaluation of the CS levels of the wild-type and the mutants (Δ*sps*, Δ*ggpS* and Δ*sps*Δ*ggpS*) confirmed the salt-induced accumulation of sucrose and GG, which is well documented in the literature [for reviews see *e.g.* Klähn and Hagemann (1), Hagemann (45),

Kirsch, Klähn (2)]. In contrast, glutamate could be detected in the absence and presence of NaCl (**Fig. 2**). These results are in agreement with the reported accumulation of this amino acid in *Synechocystis* grown in artificial seawater medium (ASW; 340 mM NaCl), and in BG11 supplemented with 12 mM KCl (40, 46).

Previous works have also reported a tradeoff between the pools of different compatible solutes and other carbon sinks, such as glycogen or extracellular polymeric substances (EPS) in cyanobacteria (47-49). In our work, the total carbohydrate content of *Synechocystis* WT and CS-deficient mutants remained unchanged when cells were exposed to NaCl, whereas a significant decrease in glycogen was observed (**Fig. 3**). Concomitantly, the accumulation of capsular polysaccharides (CPS) was observed in a salinity-dependent manner and for the strains tested. In line with these observations is the increase in the levels of proteins involved in glycogen degradation, reported when *Synechocystis* cells were grown in ASW medium (46). The protective role of EPS against salt stress was also demonstrated in a *Synechocystis* Δ*sll1581*Δ*slr1875* double mutant, showing that a decrease in CPS content increases NaCl sensitivity (50). Altogether, these results strongly suggest that under saline conditions, *Synechocystis* breaks down glycogen and redirects carbon fluxes toward the production of CS and extracellular polysaccharides, promoting cell homeostasis and contributing to cell protection.

From the three *Synechocystis* CS-deficient mutants generated in this work, the Δ*sps* was the only one able to grow in 5% NaCl. We also observed that this mutant's growth gets impaired over time, suggesting that the presence of sucrose is of additional importance for long-term cultivation. Accordingly, a previous work showed that Δ*sps* cells in stationary phase were unable to survive a salt shock, which was not observed for cells in exponential phase; this effect could be prevented by sucrose supplementation (51). Moreover, we show that the absence of sucrose leads to a severe reduction in the accumulation of GG whereas the released polysaccharides (RPS) increase significantly (1.8-fold), implying that extracellular polysaccharides production is crucial for the survival of the Δ*sps* mutant under 5% NaCl. Most importantly, our results suggest that sucrose role goes beyond osmoprotection, being involved in the regulation of metabolic pathways, e.g. triggering signaling cascades, as it was previously hypothesized by Desplats, Folco (51). For the

415 Δ*ggpS* mutant an increased sucrose level was detected under 3% NaCl, showing that this sugar
416 can sustain *Synechocystis'* survival under sea salt conditions for at least 16 days. Previously,
417 Miao, Wu (52) generated a *Synechocystis* Δ*agp* mutant unable to synthesize ADP-glucose (a
418 precursor required for GG synthesis) that was also shown to accumulate high levels of sucrose
419 and could survive upon a salt shock of 900 mM (5.2% NaCl). Notably, in the latter work and here,
420 the mutant's sucrose levels were similar to GG accumulated in the WT cultivated under the same
421 conditions. Taken together, these studies imply that GG and sucrose can have comparable
422 osmoprotectant capacity when accumulated in similar levels. Additionally, the Δ*sps*Δ*ggpS* mutant
423 was unable to survive in any salt concentration tested and glutamate was the only CS that could
424 be detected. Thus, this amino acid seems to have a minor contribution to the salt acclimation
425 process in *Synechocystis*, similar to what was reported for the halophilic bacterium *Salinibacter*
426 *ruber* (53).
427 Considering the metabolic model simulation, a synthetic device for the production of glycine
428 betaine (GB) was designed and implemented into the *Synechocystis* wild-type and our customized
429 chassis (CS-deficient mutants). Besides the ORFs required for GB production (*gsmt* and *dmt*) and
430 *metX* (to prevent SAM shortage), this device comprises well-characterized regulatory elements:
431 the synthetic promoter $P_{trc.x.lacO}$ (43), the RBS BBa_B0030, and the double terminator
432 BBa_B0015. This design ensured the stable constitutive transcription observed for the GB device
433 ORFs, regardless of the chassis or salinity conditions (**Fig. 7**), reinforcing that the use of
434 orthogonal regulatory components is crucial to ensure the proper insulation of synthetic devices
435 from the regulatory network of the chassis (54). Unlike transcription, the synthesis of the solute
436 was not independent of cultivation conditions, and GB levels increased with salinity. In
437 agreement, higher levels of glycine have been reported for *Synechocystis* cells grown in ASW
438 medium compared with those grown in BG11 (46). Since this amino acid is a precursor of GB,
439 the high levels of glycine under salinity conditions most probably favor the synthesis of GB. In
440 addition, glycogen degradation and carbon fluxes redirection toward the production of CS could
441 also explain the increased amount of GB produced in the presence of NaCl.

The implementation of the GB device into *Synechocystis* wild-type led to a small decrease in growth in all conditions tested (**Fig. 6**). As predicted by the metabolic flux model, the device may drain the cell's resources imposing a metabolic burden, causing growth impairment. This can be explained by the redirection of part of the photosynthetically fixed carbon to the synthesis of CS, which is no longer available for biomass formation, similarly to what was reported for the production of mannitol (55). In contrast to what was observed for the WT, the introduction of the GB device into the Δ*ggpS* mutant resulted in an increased salt tolerance with the concomitant growth improvement, enabling its survival under 5% NaCl. This phenotype was maintained under long-term cultivation periods up to 25 days (data not shown), suggesting that GB can compensate for the absence of GG. Conversely, the implementation of the GB device in the Δ*sps*Δ*ggpS* mutant did not improve its performance under salinity conditions. However, it remains unclear if this outcome is due to: i) insufficient production of glycine betaine to allow cell survival or ii) the absence of both native compatible solutes (sucrose and GG).

In terms of production, the highest GB amount was obtained for the Δ*ggpS* cultivated in BG11 supplemented with 3% NaCl for 4 days (1.89 μmol GB/mg protein, corresponding to 64.29 μmol/gDW) (**Fig. 8B**). Moreover, extending the cultivation period up to 16 days does not seem to affect the synthesis of GB in any condition tested (**Fig. S7**), suggesting that the process is stable. The production of GB using native organisms and heterologous hosts (with the synthesis of the solute mainly based on the metabolic pathway described for *A. halophytica*), has been previously reported (**Table 1**). However, a direct comparison is difficult since different normalization methods were used, and the cultivation conditions/time periods need also to be taken into consideration. Generally, the use of native GB producers such as the hypersaline cyanobacterium *A. halophytica* can render high amounts of the solute. This entails major disadvantages related to the high salt concentrations required, such as the reduced durability of the bioreactors, long processes, and detrimental impact on the environment. In contrast, with heterologous hosts the salinity concentrations used are at least 1/3 of those employed for *A. halophytica* (**Table 1** - heterologous production). Considering the photoautotrophic organisms, the amounts obtained using plants are low and require rather long cultivation periods. The most promising results were

obtained using the filamentous cyanobacterium *Anabaena doliolum* that produced 12.92 µmol GB per gDW after 10 days of cultivation (56). Using our *Synechocystis* Δ*ggpS* chassis, we report a production level ~5-fold higher than that of *A. doliolum* in just 4 days of cultivation (64.29 µmol GB per gDW). Regarding the heterotrophic chassis, the GB amounts obtained using different *Escherichia coli* strains were only up to 1.25-fold higher than with *Synechocystis* Δ*ggpS*. Cultivation times are significantly reduced for heterotrophic bacteria, but the use of photoautotrophic chassis enables CO_2 fixation promoting bio-mitigation and surpassing the need to supply a carbon source. Additionally, the highest GB production by our *Synechocystis* Δ*ggpS* chassis was achieved under 510 mM NaCl, opening up the possibility of large-scale cultivation with seawater (salinity range 3.1-3.8%). This does not seem as viable with *E. coli* since increasing the salt concentration to 500 mM has a substantial detrimental impact on the GB production (57).

Table 1. Native and heterologous production of glycine betaine via the three-step glycine methylation pathway.

Native production					
Strain		**Salinity (mM)**	**Production capacity**	**Cultivation time**	**Reference**
Aphanothece halophytica		2000	0.06 µmol/mg protein	1 h	(58)
Aphanothece halophytica		2000	~0.4 µmol/10^7 cells	7 days	(59)
Aphanothece halophytica		1500	~40000 µmol/gFW	10 days	(60)
Aphanothece halophytica		2000	20.1 µmol/gFW	15 days	(61)
Heterologous production					
Production strain	**Native strain**	**Salinity (mM)**	**Production capacity**	**Cultivation time**	**Reference**
Arabidopsis thaliana	*Aphanothece halophytica*	100	~2 µmol/gFW	15 days	(62)
Nicotiana tabacum	*Aphanothece halophytica*	0	0.4 µmol/gFW	28 days	(63)
Synechococcus sp. PCC 7942	*Aphanothece halophytica*	500	~1.5 µmol/gFW	NA	(62)
Anabaena sp. PCC 7120	*Aphanothece halophytica*	140	0.04 µmol/gFW	7 days	(57)
Anabaena doliolum	*Aphanothece halophytica*	500	12.92 µmol/gDW	10 days	(56)
***Synechocystis* sp. PCC 6803**	***Aphanothece halophytica***	**510**	**64.29 µmol/gDW**	**4 days**	**This work**
Escherichia coli XL1-Blue	*Ectothiorhodospira halochloris*	300	78 µmol/gDW	NA	(7)
Escherichia coli BL21	*Aphanothece halophytica*	300	~23 µmol/gDW	3 h	(6)

Escherichia coli BL21	*Aphanothece halophytica*	300	~2000 µmol/mg protein	3 h	(60)
Escherichia coli BL21	*Aphanothece halophytica*	300	~80 µmol/L	2 h	(63)
Escherichia coli DH5α	*Aphanothece halophytica*	500	6 µmol/gDW	24 h	(57)
Escherichia coli DH5α	*Aphanothece halophytica*	0	80.62 µmol/gDW	ON	(56)
Pseudomonas denitrificans	*Aphanothece halophytica*	0	NA*	1 day	(64)

ON – overnight; NA – Not available; DW – Dry weight; FW – Fresh weight; * – Identified by HPLC-MS.

Conclusions

The heterologous production of the compatible solute glycine betaine (GB) was successfully achieved in different *Synechocystis*-based chassis. The characterization of these compatible solutes (CS) deficient chassis (Δ*sps*, Δ*ggpS*, and Δ*sps*Δ*ggpS*) revealed that under saline conditions, the carbon fluxes are redirected from the synthesis of glycogen toward the production of CS and extracellular polysaccharides. In fact, the maximum amount of GB was obtained in Δ*ggpS* harboring the GB device, under 3% NaCl (64.29 µmol/gDW). This production level is promising and not far from applications using *E. coli*. Considering that the knowledge generated by the characterization of the CS deficient mutants will allow the identification of potential targets to optimize our chassis, that our GB production is based on sunlight and CO_2 fixation, and that there is the possibility of using seawater, *Synechocystis* emerges as a feasible photoautotrophic chassis for large-scale heterologous production of GB or other CS.

Materials

Reagents and enzymes

The media components and other reagents were obtained from Fisher Scientific (USA), Merck (Germany) or Sigma Aldrich (USA), and noble agar from Difco (USA). All DNA-modifying enzymes and polymerases were purchased from Thermo Fisher Scientific (USA) and Promega (USA), and standard molecular biology kits were obtained from NZY Tech (Portugal). The Sanger sequencing and oligo synthesis services were provided by STAB VIDA, Lda. (Portugal).

507

508 **Organisms and Culture Conditions**

509 Wild-type and mutants of the unicellular, non-motile cyanobacterium *Synechocystis* sp. PCC
510 6803 substrain GT-Kazusa (65, 66) (obtained from the Pasteur Culture Collection, France) were
511 maintained in Erlenmeyer flasks batch cultures with BG11 medium (67) at 30 ºC with orbital
512 shaking (150 rpm) under a 12 h light / 12 h dark regimen. Light intensity was 25 µE/m^2/s in all
513 experiments and Cosine-corrected irradiance was measured using a Dual Solar/Electric Quantum
514 Meter (Spectrum Technologies, Inc.; USA). For solid BG11, the medium was supplemented with
515 1.5% (wt/vol) noble agar, 0.3% (wt/vol) sodium thiosulfate and 10 mM TES-KOH buffer, pH 8.2
516 (67). For the selection and maintenance of mutants, BG11 medium was supplemented with
517 chloramphenicol (Cm, 10-20 µg/mL). For cloning purposes, *E. coli* strains DH5α and XL1-blue
518 were used. Cells were grown at 37 ºC in LB medium (68), supplemented with kanamycin (Km,
519 50 µg/mL) or Cm (34 µg/mL).

520

521 **DNA and RNA extraction**

522 Cyanobacterial genomic DNA (gDNA) extraction was performed according to the procedure
523 described previously (69). For RNA extraction, 50 mL of *Synechocystis* culture at $OD_{730} \approx 1$ was
524 centrifuged for 10 min at 4,470 *g*; cell pellets were treated with RNAprotect Bacteria Reagent
525 (Qiagen, Germany) according to instructions, and stored at -80 °C. RNA was extracted using the
526 TRIzol® Reagent (Ambion) according to the method described previously (70) with the following
527 adaptations: the cells were disrupted using a FastPrep®-24 (MP Biomedicals) in 2 cycles of 1 min
528 at 4.0 m/s and the RNA samples were treated with 1 U of RQ1 RNase-Free DNase (Promega)
529 according to manufacturer's instructions.

530

531 **Glycine betaine device: Design, DNA synthesis and assembly**

532 The synthetic construction for the synthesis of glycine betaine (Ahbet) was designed based on
533 *gsmt* (encoding the glycine-sarcosine-N-methyltransferase) and *dmt* (encoding the
534 dimethylglycine-N-methyltransferase) Open Reading Frames (ORFs) from the cyanobacterium

Aphanothece halophytica, and the *metX* (*sll0927*, encoding S-adenosyl-methionine synthase) ORF from *Synechocystis*. All the ORF sequences were codon optimized for *Synechocystis* using the Gene Designer 2.0 software (DNA 2.0, Inc.; USA), restriction sites incompatible with the BioBrick™ standard RFC[10] were eliminated and double stop codons included. Each ORF is preceded by the BioBrick™ (BB) ribosome binding site (RBS) BBa_B0030 and the double terminator BBa_B0015 was included after the *metX* ORF. In addition, the synthetic construction is flanked by the prefix and suffix sequences of the BB RFC[10] standard. All the BB sequences were retrieved from the Registry of Standard Biological Parts (parts.igem.org). Subsequently, the sequence of the glycine betaine synthetic construction flanked by the BB prefix, the double terminator and BB suffix was synthesized and cloned into *Sma*I digested pBluescript II SK(-) (Epoch Life Science, Inc.; USA).

To construct the glycine betaine device, the synthesized Ahbet construct was assembled with the synthetic promoter $P_{trc.x.lacO,}$ previously characterized in *Synechocystis* (43). For this purpose, the Ahbet was PCR-amplified from the plasmid pBSK with the pUC primers (**Additional file 1: Table S4**), using Phusion high-fidelity DNA polymerase, according to the manufacturer's instructions. The PCR product was purified using NZYGelpure kit, digested with *Xba*I and *Pst*I and cloned downstream of $P_{trc.x.lacO}$ in the pJ201 plasmid (digested with *Spe*I and *Pst*I, and dephosphorylated). The generated $P_{trc.x.lacO}$::Ahbet device was excised from the pJ201 plasmid with *Xba*I and *Spe*I, and transferred to pSEVA351 shuttle vector (obtained from the "Standard European Vector Architecture" repository (71)), digested with *Xba*I. The assembly and transfer of the synthetic device was confirmed by PCR, restriction analysis and Sanger sequencing.

Construction of integrative plasmids for the generation of CS mutants

The construction of integrative plasmids for the knockout of *ggpS* and *sps* genes was performed as described previously (72). Briefly, the plasmids were based on pGEM-T® Easy (Promega, USA) and contain the *Synechocystis* chromosomal regions flanking the *ggpS* or the *sps* gene. The 5'- and 3'-flanking regions were amplified from the cyanobacterium's genome using *Pfu* DNA polymerase and the primer pairs 5-O/5-I and 3-O/3-I (**Additional file 1: Table S4**), respectively.

563 Subsequently, the purified PCR fragments were fused by Overlap Extension PCR using primers
564 5-O/3-O and 80 ng of each amplicon. The resulting product was purified and cloned into the
565 vector pGEM-T® Easy, according to the manufacturer's instructions, originating the pGDggpS
566 and the pGDsps plasmids (**Table 2**). A selection cassette, containing the *nptII* gene (conferring
567 resistance to neomycin and kanamycin) and the *sacB* gene (conferring sensitivity to sucrose), was
568 PCR amplified from the plasmid pK18mobsacB (73) with specific primers (**Additional file 1:**
569 **Table S4**). The amplicon was then cloned into the *Age*I/SmaI restriction site of pGDggpS or
570 pGDsps plasmids, generating the pGDggpS.KS and the pGDsps.KS plasmids, respectively
571 (**Table 2**). All constructs were confirmed by sequencing.
572
573 **Table 2 - List of plasmids used to transform *Synechocystis.***

Designation	Plasmid	Description	Reference/ Source
$P_{trc.x.lacO}$::Ahbet	pSEVA351	Ahbet synthetic construction under the control of the $P_{trc.x.lacO}$ promoter	This study
pGDggpS	pGEM-T® Easy	pGEM-T easy vector containing the two regions for double homologous recombination targeting the *ggpS locus*	(43)
pGDggpS.KS	pGEM-T® Easy	pGEM-T easy vector containing the *nptII* and *sacB* genes flanked by the two regions for double homologous recombination targeting the *ggpS locus*	This study
pGDsps	pGEM-T® Easy	pGEM-T easy vector containing the two regions for double homologous recombination targeting the *sps locus*	This study
pGDsps.KS	pGEM-T® Easy	pGEM-T easy vector containing the *nptII* and *sacB* genes flanked by the two regions for double homologous recombination targeting the *sps locus*	This study

574
575 **Generation of *Synechocystis* CS knockout mutants**
576 *Synechocystis* was transformed based on the protocol described by Williams (74) with
577 modifications. *Synechocystis* cultures were grown under standard conditions to an $OD_{730} \approx 0.5$.
578 Cells were harvested by centrifugation at 3,850 *g* for 10 min; and then resuspended in BG11 to a
579 final $OD_{730} \approx 2.5$. A 500 µL aliquot of these cells was used (per transformation) and incubated
580 with purified pGDggpS.KS or pGDsps.KS plasmids, at a final DNA concentration of 20 µg/mL,
581 for 5 h in light at 30 °C. Cells were then spread onto Immobilon™-NC membranes (0.45 µm pore

size, 82 mm, Millipore, USA) resting on solid BG11 plates, incubated at 25 °C under low light, and transferred to selective solid BG11 plates supplemented with 10 µg/mL Km after 24 h. Transformants were observed after 1-2 weeks. For complete segregation, Km-resistant colonies were streaked on BG11 plates with increasing Km concentrations (up to 500 µg/mL), and finally transferred into liquid medium. Mutants were then tested for sucrose sensitivity and confirmed by PCR and Southern blot (for details see below). Subsequently, to remove the selection markers from the insertion mutants, cells were transformed as described above with the pGDggpS or the pGDsps plasmids, and the mutants were selected on solid BG11 containing 10% (wt/vol) sucrose. These mutants were also screened for Km-sensitivity. The double mutant Δ*sps*Δ*ggpS* was generated by deleting the *ggpS* gene from the Δ*sps* background following the abovementioned protocol. The full segregation of the mutants was confirmed by PCR using GoTaq® G2 Flexi DNA Polymerase, together with specific primers (**Additional file 1: Table S4**), according to manufacturer's instructions. Mutant segregation was also confirmed by Southern blots that were performed using 4 µg of genomic DNA of the wild-type and mutants, digested with *Mun*I (wild-type, Δ*sps.KS*, Δ*sps*, Δ*ggpS.KS* and Δ*ggpS*), and *Ava*II (wild-type, Δ*sps*Δ*ggpS.KS* and Δ*sps*Δ*ggpS*). The DNA fragments were separated by electrophoresis on a 1% (wt/vol) agarose gel and blotted onto Hybond™-N membrane (GE Healthcare, USA). Probes covering the 5' flanking region of the *ggpS* or 3' flanking region of the *sps* genes were amplified by PCR (using primers indicated in **Additional file 1: Table S4**), and labeled using the DIG DNA labelling kit (Roche Diagnostics GmbH, Germany), according to the manufacturer's instructions. Hybridization was performed overnight at 65 °C, and digoxigenin-labelled probes were detected by chemiluminescence using CPD-star (Roche) in a Chemi Doc™ XRS+ Imager (Bio-Rad, USA).

Introduction of the glycine betaine synthetic device into *Synechocystis*

The pSEVA351 plasmid containing the synthetic device $P_{trc.x.lacO}$::Ahbet (**Table 2**) was introduced into *Synechocystis* by electroporation following the protocol described previously (43). The presence of the synthetic device was confirmed in *Synechocystis* transformants by PCR using specific primers (**Additional file 1: Table S4**), as described by Ferreira, Pacheco (43).

610

611 **Growth experiments**

612 Pre-cultures of *Synechocystis* wild-type and mutants were inoculated in BG11 medium
613 (supplemented with 10 μg/mL Cm, when appropriate) and grown in an orbital shaker (150 rpm),
614 at 30 ºC under a 12 h light (25 $\mu E/m^2/s$) / 12 h dark regimen. The cultures were grown to an OD_{730}
615 ≈ 2 and, subsequently, diluted in fresh BG11 medium without antibiotic to a final $OD_{730} \approx 0.5$.
616 Fifty milliliters of the dilution were transferred to 100 mL Erlenmeyer flasks without NaCl or
617 containing 3%, 5%, or 7% (wt/vol) NaCl (510, 860 and 1200 mM NaCl, respectively), previously
618 sterilized. These cultures were maintained in the same conditions as the pre-cultures and growth
619 was monitored for at least 16 days, by measuring the optical density at 730 nm (OD_{730}) and
620 determining the chlorophyll *a* (chl *a*) content as described by Meeks and Castenholz (75). All the
621 growth experiments included, at least, three biological replicates with technical duplicates.
622

623 **Total carbohydrate content, released and capsular polysaccharides (RPS and CPS)**
624 **measurements**

625 Total carbohydrate content and RPS were determined as previously described (76). Briefly, 10
626 mL of culture samples were dialyzed (12–14 kDa molecular weight cutoff; CelluSepT4, Orange
627 Scientific) against at least 10 volumes of distilled water, 3% or 5% (wt/vol) NaCl solutions
628 (identical to the growth medium), for at least 24 h. One milliliter of the collected sample was used
629 to spectrophotometrically quantify the total carbohydrate content by the phenol-sulfuric acid
630 method (77), whereas 5 mL of the dialyzed sample was centrifuged at 3,857 *g* for 10 min at RT,
631 and the cell-free supernatant was used to determine the RPS. For CPS quantification, the
632 procedure was performed as described previously (78). Five milliliters of dialyzed cultures were
633 centrifuged at 3,857 *g* for 10 min at RT, the cell pellet was resuspended in water and boiled for
634 15 min. After centrifugation as described previously, the cell-free supernatant was used for CPS
635 measurement by the phenol-sulfuric acid method (77). Total carbohydrate content, RPS and CPS
636 were normalized by chl *a* content. All experiments included, at least, three biological replicates
637 with technical triplicates.

638

639 **Glycogen extraction and quantification**

640 Glycogen extraction was performed as described previously (79). Ten milliliters of cell culture
641 were centrifuged, and the cell pellet was suspended in 100 µL of distilled water and 400 µL of
642 30% (wt/vol) KOH was added. The mixture was incubated at 100 ºC for 90 min and then quickly
643 cooled on ice. Six hundred µL of ice-cold absolute ethanol were added, and the mixture was
644 incubated on ice for 2 h. The mixture was centrifuged for 5 min at maximum speed and 4 ºC. The
645 supernatant was discarded, and the isolated glycogen was washed three times with 500 µL of ice-
646 cold absolute ethanol and dried at 60 ºC. Glycogen quantification was performed by the phenol-
647 sulfuric acid method (77), and normalized by chl *a* content. Experiments included, at least, three
648 biological replicates with technical triplicates.

649

650 **Optical microscopy**

651 Cultures of *Synechocystis* wild-type (WT) and the Δ*sps* mutant were grown in BG11 or BG11
652 supplemented with 5% (wt/vol) NaCl as stated above (initial $OD_{730} \approx 0.5$). Four days after
653 inoculation, cells were stained with 0.5% (wt/vol) of Alcian Blue (in 3% (vol/vol) acetic acid) in
654 1:1 (culture:dye) ratio. This mixture was added to 10 µL of 1% (wt/vol) low-melting point agarose
655 beds (dissolved in BG11 medium) and covered with a coverslip. The preparations were observed
656 using the light microscope Olympus DP25 Camera software Cell B.

657

658 **Transcription Analysis by RT-qPCR**

659 After extraction (for details see above), RNA concentration and purity (the ratios A_{260}/A_{280} and
660 A_{260}/A_{230}) were measured using a NanoDrop ND-1000 spectrophotometer (NanoDrop
661 Technologies, Inc.; USA). The quality and integrity of the RNA samples was also inspected in
662 1% (wt/vol) agarose gel performed by standard protocols using TAE buffer. The absence of
663 genomic DNA contamination was checked by PCR, in reaction mixtures containing 0.5 U of
664 GoTaq® G2 Flexi DNA Polymerase, 1x Green GoTaq Flexi buffer, 200 µM of each dNTP, 1.5
665 mM $MgCl_2$, 0.25 µM of each rnpB primer (**Additional file 1: Table S4**), and 200 ng of total

RNA. The PCR profile was: 5 min at 95 °C followed by 25 cycles of 20 s at 95 °C, 20 s at 56 °C and 20 s at 72 °C, and a final extension at 72 °C for 5 min. The PCR reactions were run on 1% (wt/vol) agarose gel as described above. For cDNA synthesis, 1 µg of total RNA was transcribed with the iScript™ Reverse Transcription Supermix for RT-qPCR (Bio-Rad) in a final volume of 20 µL, following the manufacturer's instructions. A control PCR was performed using 1 µL of cDNA as a template, the BD16S primers (**Additional file 1: Table S4**), and the same reaction conditions and PCR program described above. Five-fold standard dilutions of the cDNAs were made (1/5, 1/25, 1/125 and 1/625) and stored at -20 °C. RT-qPCRs were performed on Hard-Shell 384-Well PCR Plates (thin wall, skirted, clear/white) covered with Microseal® B adhesive seal (Bio-Rad). The reactions (10 µl) were manually assembled and contained 0.125 µM of each primer (**Additional file 1: Table S4**), 5 µL of iTaq™ Universal SYBR® Green Supermix (Bio-Rad) and 1 µL of template cDNA (dilution 1/5). The PCR protocol used was: 3 min at 95 °C followed by 45 cycles of 30 s at 95 °C, 30 s at 56 °C and 30 s at 72 °C. In the end, a melting curve analysis of the amplicons (10 s cycles between 55-95 °C with a 0.5 °C increment per cycle) was conducted. Standard dilutions of the cDNA were used to check the relative efficiency and quality of primers, and negative controls (no template cDNA) included (for more details on RT-qPCR parameters see **Additional file 1: Table S5**). RT-qPCRs were performed with three biological replicates and technical triplicates of each cDNA sample in the CFX384 Touch™ Real-Time PCR Detection System (Bio-Rad). The data obtained were analyzed using the Bio-Rad CFX Maestro™ 1.1 software, implementing an efficiency-corrected delta Cq method (ΔCq). This method was used since the target genes *gsmt*, *dmt* and *metX* were validated as reference genes using the reference gene selection tool available in the Maestro™ software. For this reason, the relative expression of the targets is represented instead of the usual relative normalized expression. Statistical analysis was performed using a one-way ANOVA using the same software, and tests were considered significant if $P < 0.05$. The amplicon sizes were checked by agarose gel electrophoresis, and the DNA sequence was confirmed by Sanger sequencing. These experiments were compliant with the MIQE guidelines (80), to promote the effort for experimental consistency and transparency, and to increase the reliability and integrity of the results obtained.

694

695 **Compatible solutes (CS) quantification**

696 Cultures of *Synechocystis* wild-type (WT), the Δ*sps*, Δ*ggpS* and Δ*sps*Δ*ggpS* mutants and the
697 strains harboring the GB device (WT, Δ*ggpS* and Δ*sps*Δ*ggpS* backgrounds) were grown in BG11
698 or BG11 supplemented with 3% or 5% (wt/vol) NaCl, as described above, at an initial $OD_{730} \approx$
699 0.5. The quantification of the CS – sucrose, glutamate, glucosylglycerol and glycine betaine –
700 was performed using 500 mL culture (distributed in 50 mL cultures in 100 mL Erlenmeyer flasks).
701 Four days after inoculation, cells were harvested by centrifugation at 4,470 *g* for 10 min at room
702 temperature (RT). In the case of the strains harboring the GB device, the extracellular medium
703 was stored at -80 ºC, for further lyophilization and CS extraction. Cells were washed using 100
704 mL of cold distilled water, 3% or 5% (wt/vol) NaCl solutions (identical to the growth medium).
705 Centrifugation was repeated and the cell pellets were resuspended in 50 mL of the respective
706 solutions. From this suspension, a 0.5 mL aliquot was centrifuged and stored at -20 ºC to be used
707 later for protein quantification. The remaining cell suspension was centrifuged at 4 ºC and the cell
708 pellet was stored at -20 ºC. Ethanol-chloroform extraction of the CS was performed as described
709 in Ferreira, Pacheco (43) with adaptations. Briefly, cell pellets or lyophilized extracellular
710 medium were suspended in 25 mL of 80% (vol/vol) ethanol and subsequently transferred to a 100
711 mL round flask containing a magnetic stir bar. The flask was connected to a coil condenser
712 (circulating cold water) and heated at 100 ºC with stirring, for 10 min. The suspension was
713 transferred to a 50 mL tube and centrifuged at 4,000 *g* for 10 min at RT. The supernatant was
714 stored and the pellet resuspended in 20 mL of 80% (vol/vol) ethanol for a new extraction process.
715 The remainder protocol was performed as described in (81). Detection, identification and
716 quantification of CS was performed by proton NMR. To that effect, freeze-dried extracts were
717 dissolved in 1 mL of D_2O and a known amount of sodium formate was added to serve as an
718 internal concentration standard. Spectra were acquired at 25 ºC on a Bruker Avance *III* 800
719 spectrometer (Bruker, Rheinstetten, Germany) working at a proton operating frequency of 800.33
720 MHz, equipped with a 5 mm, three channel, inverse detection cryoprobe TCI-z H&F/C/N with
721 pulse-field gradients. A 3 s soft pulse was applied before the excitation pulse, to pre-saturate the

water signal. Spectra were acquired under fully relaxed conditions (flip angle 60º; repetition delay of 60 s) so that the area of the NMR signals was proportional to the amount of the different protons in the sample. Integration of the signals was performed using the tools available in the TopSpin software (Bruker, Rheinstetten, Germany) version 3.6.2. The concentration of CS was expressed as µmol per mg of protein. Protein extracts were obtained by sonication as described by Pinto, Pacheco (37), and protein quantification was performed using the Bio-Rad Protein Assay. For cell dry weight (DW) determinations, 40 mL of culture at $OD_{730} \approx 1.0$ (or equivalent) was centrifuged at 3,857 *g* for 10 min at RT. Then, the cell pellet was dried at 60 °C for 48 h. Experiments included, at least, three biological replicates.

In silico **analysis of CS production**

The genome-scale metabolic model of *Synechocystis* – *i*Syn811 (33) –, was updated to include all the information required for the simulations. The manual curation process started with the addition of the final reaction in the synthesis of sucrose ("spp: H_2O + sucrose 6-phosphate → phosphate + sucrose"), and also the metabolic precursors and the three reactions required for the synthesis of the heterologous CS, glycine betaine ("GSMT1: *S*-adenosyl-L-methionine + glycine ↔ *S*-adenosyl-L-homocysteine + sarcosine", "GSMT2: *S*-adenosyl-L-methionine + sarcosine ↔ *S*-adenosyl-L-homocysteine + *N,N*-dimethylglycine" and "DMT: *S*-adenosyl-L-methionine + *N,N*-dimethylglycine ↔ *S*-adenosyl-L-homocysteine + *N,N,N*-trimethylglycine"). In this process, the nomenclature was corrected and standardized (e.g. "glycerone" to "dihydroxy-acetone" or "GDP-mannose" to "GDP-D-mannose"), and the reversibility of some reactions changed (e.g. "sn-glycerol-3-phosphate → dihydroxy-acetone phosphate" to "sn-glycerol-3-phosphate ↔ dihydroxy-acetone phosphate"). Flux balance analysis (82) was performed to the *i*Syn811 genome-scale metabolic reconstruction of *Synechocystis* for the production assessment of four different CS: three heterologous (glycine betaine, ectoine and mannosylglycerate), and three native (glucosylglycerol, glutamate and sucrose). The MATLAB software, COBRA Toolbox v3.0 (41) was used for quantitative prediction of cellular and multicellular biochemical networks with constraint-based modelling. Simulations were constrained to match an autotrophic specific

growth rate of 0.09/h, which corresponds to a light input of 0.8 mE/gDW/h and to a net carbon flux of 3.4 mmol/gDW/h into the cell, with CO_2 as carbon source. The description of the *i*Syn811 model and further information on the simulation procedure are available in Montagud, Navarro (32).

Statistical analysis

The statistical analysis was performed by means of one- or two-way ANOVAs, using GraphPad Prism v6.01 (GraphPad Software Inc., USA).

List of abbreviations

CPS: capsular polysaccharides; CS: compatible solutes; DW: dry weight; EPS: extracellular polymeric substances; FW: fresh weight; GB: glycine betaine; GG: glucosylglycerol; NMR: nuclear magnetic resonance; ORF: open reading frame; RBS: ribosome binding site; RPS: released polysaccharides; RT: room temperature; RT-qPCR: quantitative reverse transcription; WT: wild-type.

Supplementary information

The online version contains supplementary material available at XX.

Additional file 1: **Fig. S1 -** Confirmation of knockout mutants by PCR. **Fig. S2 -** Confirmation of knockout mutants by Southern blot. **Fig. S3 -** H-NMR spectra for compatible solutes quantification in the WT and knockout mutants. **Fig. S4 -** Theoretical productivity of heterologous compatible solutes. **Fig. S5 -** Confirmation of the presence of the glycine betaine device by PCR. **Fig. S6 -** Growth curves of the strains harboring the glycine betaine device. **Fig. S7 –** Compatible solutes quantification in Δ*ggpS* $P_{trc.x.lacO}$::Ahbet after 4 and 16 days of cultivation. **Fig. S8 -** H-NMR spectra for compatible solutes quantification in the strains harboring the glycine betaine device. **Table S1 -** Analysis of growth decrease under salinity conditions. **Table S2 -** Relative expression data of *gsmt, dmt* and *metX* (RT-qPCR). **Table S3 -** Quantification of glycine betaine

in the extracellular medium. **Table S4 -** List of the PCR primers used in the study. **Table S5 -** Amplicon and RT-qPCR reaction parameters. **References**

DECLARATIONS

Ethics approval and consent to participate

Not applicable.

Consent for publication

Not applicable.

Availability of data and materials

The raw data and the research material described in the article are available on request.

Competing interests

The authors have no conflict of interests to declare.

Funding

This work was financed by Portuguese funds through the Fundação para a Ciência e a Tecnologia (FCT)/Ministério da Ciência, Tecnologia e Ensino Superior within the scope of UIDB/04293/2020 and UIDP/04293/2020. We also greatly acknowledge FCT for the scholarship SFRH/BD/117508/2016 (EAF) and the Assistant Researcher contracts CEECIND/00259/2017 (CCP) and 2020.01953.CEECIND (FP). The NMR data were acquired at CERMAX, ITQB-NOVA, Oeiras, Portugal with equipment funded by FCT, project AAC 01/SAICT/2016.

Authors' contributions

CCP, EAF, FP and PT were involved in the conceptual design of the work. The experimental design and strain engineering were carried out by EAF, CCP, JSR and FP. Characterization and data analysis were performed by EAF and CCP. CS quantification by proton NMR was carried out by PL. EAF, DF and JFU were involved in the curation, simulations and analyses involving the *i*Syn metabolic model. Data interpretation and manuscript preparation was performed by EAF, CCP, DF (*i*Syn metabolic model) and PT. All authors have revised and approved the submitted version of the manuscript.

Acknowledgements

The authors acknowledge the technical and scientific support of the i3S Scientific Platform "Cell Culture and Genotyping" in the RT-qPCR experiments. We are grateful to: Prof. Paula Gomes, Dr. Luísa Aguiar and Mélanie Fonte (LAQV-REQUIMTE, Faculdade de Ciências, Universidade do Porto) for providing the equipment and technical assistance regarding compatible solutes extraction; Dr. Paulo Oliveira (i3S) for all the support provided, the scientific discussions and suggestions; and Dr. Maria Siurana (UPV) for the scientific discussions regarding the *i*Syn metabolic model.

References

1. Klähn S, Hagemann M. Compatible solute biosynthesis in cyanobacteria. Environ Microbiol. 2011;13:551-62.
2. Kirsch F, Klähn S, Hagemann M. Salt-regulated accumulation of the compatible solutes sucrose and glucosylglycerol in cyanobacteria and its biotechnological potential. Front Microbiol. 2019;10:2139.
3. Landfald B, Strøm AR. Choline-glycine betaine pathway confers a high level of osmotic tolerance in *Escherichia coli*. J Bacteriol. 1986;165:849-55.
4. Rathinasabapathi B, Burnet M, Russell BL, Gage DA, Liao P-C, Nye GJ, et al. Choline monooxygenase, an unusual iron-sulfur enzyme catalyzing the first step of glycine betaine synthesis in plants: Prosthetic group characterization and cDNA cloning. PNAS. 1997;94:3454-8.
5. Grossman EB, Hebert SC. Renal inner medullary choline dehydrogenase activity: characterization and modulation. Am J Physiol - Ren Physiol. 1989;256:F107-F12.
6. Waditee R, Tanaka Y, Aoki K, Hibino T, Jikuya H, Takano J, et al. Isolation and functional characterization of *N*-methyltransferases that catalyze betaine synthesis from glycine in a halotolerant photosynthetic organism *Aphanothece halophytica*. J Biol Chem. 2003;278:4932-42.
7. Nyyssola A, Kerovuo J, Kaukinen P, von Weymarn N, Reinikainen T. Extreme halophiles synthesize betaine from glycine by methylation. J Biol Chem. 2000;275:22196-201.
8. Guinn EJ, Pegram LM, Capp MW, Pollock MN, Record MT. Quantifying why urea is a protein denaturant, whereas glycine betaine is a protein stabilizer. PNAS. 2011;108:16932-7.
9. Stadmiller SS, Gorensek-Benitez AH, Guseman AJ, Pielak GJ. Osmotic shock induced protein destabilization in living cells and its reversal by glycine betaine. J Mol Biol. 2017;429:1155-61.
10. Holmström KO, Somersalo S, Mandal A, Palva TE, Welin B. Improved tolerance to salinity and low temperature in transgenic tobacco producing glycine betaine. J Exp Bot. 2000;51:177-85.
11. You L, Song Q, Wu Y, Li S, Jiang C, Chang L, et al. Accumulation of glycine betaine in transplastomic potato plants expressing choline oxidase confers improved drought tolerance. Planta. 2019;249:1963-75.
12. Caldas T, Demont-Caulet N, Ghazi A, Richarme G. Thermoprotection by glycine betaine and choline. Microbiol. 1999;145:2543-8.
13. Cleland D, Krader P, McCree C, Tang J, Emerson D. Glycine betaine as a cryoprotectant for prokaryotes. J Microbiol Methods. 2004;58:31-8.
14. Lever M, Slow S. The clinical significance of betaine, an osmolyte with a key role in methyl group metabolism. Clin Biochem. 2010;43:732-44.

15. Day CR, Kempson SA. Betaine chemistry, roles, and potential use in liver disease. Biochim Biophys Acta. 2016;1860:1098-106.
16. Rady MO, Semida WM, Abd El-Mageed TA, Hemida KA, Rady MM. Up-regulation of antioxidative defense systems by glycine betaine foliar application in onion plants confer tolerance to salinity stress. Sci Hortic. 2018;240:614-22.
17. Sun H, Luo M, Zhou X, Zhou Q, Sun Y, Ge W, et al. Exogenous glycine betaine treatment alleviates low temperature-induced pericarp browning of 'Nanguo' pears by regulating antioxidant enzymes and proline metabolism. Food Chem. 2020;306:125626.
18. Cholewa JM, Guimarães-Ferreira L, Zanchi NE. Effects of betaine on performance and body composition: a review of recent findings and potential mechanisms. Amino Acids. 2014;46:1785-93.
19. Eklund M, Bauer E, Wamatu J, Mosenthin R. Potential nutritional and physiological functions of betaine in livestock. Nutr Res Rev. 2005;18:31-48.
20. Dikilitas M, Simsek E, Roychoudhury A. Role of proline and glycine betaine in overcoming abiotic stresses. In: Roychoudhury A, Tripathi DK, editors. Protective chemical agents in the amelioration of plant abiotic stress: biochemical and molecular perspectives: John Wiley & Sons Ltd.; 2020. p. 1-23.
21. Nsimba ZF, Paquot M, Mvumbi LG, Deleu M. Glycine betaine surfactant derivatives: Synthesis methods and potentialities of use. Biotechnol Agron Soc Envir. 2010;14:737-48.
22. Heikkila HO, Melaja JA, Millner DE, Virtanen JJ, inventors; Google Patents, assignee. Betaine recovery process patent US4359430A. 1982.
23. Kar JR, Hallsworth JE, Singhal RS. Fermentative production of glycine betaine and trehalose from acid whey using *Actinopolyspora halophila* (MTCC 263). Environ Technol Innov. 2015;3:68-76.
24. DuPont. Betafin® natural betaine sustainable and substantiated. 2015. http://animalnutrition.dupont.com/fileadmin/user_upload/live/animal_nutrition/documents/open/Betafin__Natural_Betaine_Lifecycle_Analysis.pdf. Accessed 14 Oct 2021.
25. Knoll AH. Cyanobacteria and Earth History. In: Flores FG, Herrero A, editors. The cyanobacteria: molecular biology, genomics, and evolution. Norfolk, UK: Caister Academic Press; 2008. p. 1-19.
26. Ananya AK, Ahmad IZ. Cyanobacteria" the blue green algae" and its novel applications: A brief review. IJIAS. 2014;7:251-61.
27. Hays SG, Ducat DC. Engineering cyanobacteria as photosynthetic feedstock factories. Photosynth Res. 2015;123:285-95.
28. Lindblad P. Hydrogen production using novel photosynthetic cell factories. Cyanobacterial hydrogen production: design of efficient organisms. In: Torzillo G, Seibert M, editors. Microalgal Hydrogen Production: Achievements and Perspectives. G. Royal Society of Chemistry, UK.: G. Royal Society of Chemistry, UK.; 2018. p. 323-34.
29. Sadvakasova AK, Kossalbayev BD, Zayadan BK, Bolatkhan K, Alwasel S, Najafpour MM, et al. Bioprocesses of hydrogen production by cyanobacteria cells and possible ways to increase their productivity. Renew Sustain Energy Rev. 2020;133:110054.
30. Wang L, Chen L, Yang S, Tan X. Photosynthetic conversion of carbon dioxide to oleochemicals by cyanobacteria: Recent advances and future perspectives. Front Microbiol. 2020;11:634.
31. Rodrigues JS, Lindberg P. Engineering cyanobacteria as host organisms for production of terpenes and terpenoids. In: Jens Nielsen SL, Gregory Stephanopoulos, Paul Hudson, editor. Cyanobacteria Biotechnology: WILEY-VCH GmbH; 2021. p. 267-300.
32. Montagud A, Navarro E, Fernandez de Cordoba P, Urchueguia JF, Patil KR. Reconstruction and analysis of genome-scale metabolic model of a photosynthetic bacterium. BMC Syst Biol. 2010;4:156.
33. Montagud A, Zelezniak A, Navarro E, de Cordoba PF, Urchueguia JF, Patil KR. Flux coupling and transcriptional regulation within the metabolic network of the photosynthetic bacterium *Synechocystis* sp. PCC 6803. Biotechnol J. 2011;6:330-42.

34. Joshi CJ, Peebles CA, Prasad A. Modeling and analysis of flux distribution and bioproduct formation in *Synechocystis* sp. PCC 6803 using a new genome-scale metabolic reconstruction. Algal Res. 2017;27:295-310.
35. Gopalakrishnan S, Pakrasi HB, Maranas CD. Elucidation of photoautotrophic carbon flux topology in *Synechocystis* PCC 6803 using genome-scale carbon mapping models. Metab Eng. 2018;47:190-9.
36. Heidorn T, Camsund D, Huang H-H, Lindberg P, Oliveira P, Stensjö K, et al. Synthetic biology in cyanobacteria: engineering and analyzing novel functions. In: Voigt C, editor. Methods Enzymol. 497: Academic Press; 2011. p. 539-79.
37. Pinto F, Pacheco CC, Oliveira P, Montagud A, Landels A, Couto N, et al. Improving a *Synechocystis*-based photoautotrophic chassis through systematic genome mapping and validation of neutral sites. DNA Res. 2015;22:425-37.
38. Huang HH, Camsund D, Lindblad P, Heidorn T. Design and characterization of molecular tools for a Synthetic Biology approach towards developing cyanobacterial biotechnology. Nucleic Acids Res. 2010;38:2577-93.
39. Pacheco CC, Ferreira EA, Oliveira P, Tamagnini P. Synthetic biology of cyanobacteria. In: Kourist R, Schmidt S, editors. The autotrophic biorefinery: raw materials from biotechnology. De Gruyter 2021. p. 131-71.
40. Iijima H, Watanabe A, Sukigara H, Shirai T, Kondo A, Osanai T. Simultaneous increases in the levels of compatible solutes by cost-effective cultivation of *Synechocystis* sp. PCC 6803. Biotechnol Bioeng. 2020;117:1649-60.
41. Heirendt L, Arreckx S, Pfau T, Mendoza SN, Richelle A, Heinken A, et al. Creation and analysis of biochemical constraint-based models using the COBRA Toolbox v.3.0. Nat Protoc. 2019;14:639-702.
42. Canton B, Labno A, Endy D. Refinement and standardization of synthetic biological parts and devices. Nat Biotechnol. 2008;26:787-93.
43. Ferreira EA, Pacheco CC, Pinto F, Pereira J, Lamosa P, Oliveira P, et al. Expanding the toolbox for *Synechocystis* sp. PCC 6803: validation of replicative vectors and characterization of a novel set of promoters. Synth Biol. 2018;3.
44. Kaleta C, Schäuble S, Rinas U, Schuster S. Metabolic costs of amino acid and protein production in *Escherichia coli*. Biotechnol J. 2013;8:1105-14.
45. Hagemann M. Genomics of salt acclimation: synthesis of compatible solutes among cyanobacteria. In: Franck Chauvat CC-C, editor. Adv Bot Res. 65: Academic Press; 2013. p. 27-55.
46. Iijima H, Nakaya Y, Kuwahara A, Hirai MY, Osanai T. Seawater cultivation of freshwater cyanobacterium *Synechocystis* sp. PCC 6803 drastically alters amino acid composition and glycogen metabolism. Front Microbiol. 2015;6:326.
47. Baran R, Lau R, Bowen BP, Diamond S, Jose N, Garcia-Pichel F, et al. Extensive turnover of compatible solutes in cyanobacteria revealed by deuterium oxide (D_2O) stable isotope probing. ACS Chem Biol. 2017;12:674-81.
48. Kirsch F, Pade N, Klahn S, Hess WR, Hagemann M. The glucosylglycerol-degrading enzyme GghA is involved in acclimation to fluctuating salinities by the cyanobacterium *Synechocystis* sp. strain PCC 6803. Microbiol. 2017;163:1319-28.
49. Du W, Liang F, Duan Y, Tan X, Lu X. Exploring the photosynthetic production capacity of sucrose by cyanobacteria. Metab Eng. 2013;19:17-25.
50. Jittawuttipoka T, Planchon M, Spalla O, Benzerara K, Guyot F, Cassier-Chauvat C, et al. Multidisciplinary evidences that *Synechocystis* PCC6803 exopolysaccharides operate in cell sedimentation and protection against salt and metal stresses. PLoS One. 2013;8:e55564.
51. Desplats P, Folco E, Salerno GL. Sucrose may play an additional role to that of an osmolyte in *Synechocystis* sp. PCC 6803 salt-shocked cells. Plant Physiol Biochem. 2005;43:133-8.
52. Miao X, Wu Q, Wu G, Zhao N. Sucrose accumulation in salt-stressed cells of *agp* gene deletion-mutant in cyanobacterium *Synechocystis* sp. PCC 6803. FEMS Microbiol Lett. 2003;218:71-7.

53. Oren A, Heldal M, Norland S, Galinski EA. Intracellular ion and organic solute concentrations of the extremely halophilic bacterium *Salinibacter ruber*. Extremophiles. 2002;6:491-8.
54. Costello A, Badran AH. Synthetic Biological Circuits within an Orthogonal Central Dogma. Trends Biotechnol. 2021;39:59-71.
55. Wu W, Du W, Gallego RP, Hellingwerf KJ, van der Woude AD, Dos Santos FB. Using osmotic stress to stabilize mannitol production in *Synechocystis* sp. PCC6803. Biotechnol Biofuels. 2020;13:117.
56. Singh M, Sharma NK, Prasad SB, Yadav SS, Narayan G, Rai AK. The freshwater cyanobacterium *Anabaena doliolum* transformed with *ApGSMT-DMT* exhibited enhanced salt tolerance and protection to nitrogenase activity, but became halophilic. Microbiol. 2013;159:641-8.
57. Waditee-Sirisattha R, Singh M, Kageyama H, Sittipol D, Rai AK, Takabe T. *Anabaena* sp. PCC7120 transformed with glycine methylation genes from *Aphanothece halophytica* synthesized glycine betaine showing increased tolerance to salt. Arch Microbiol. 2012;194:909-14.
58. Ishitani M, Takabe T, Kojima K, Takabe T. Regulation of glycinebetaine accumulation in the halotolerant cyanobacterium *Aphanothece halophytica*. Funct Plant Biol. 1993;20:693-703.
59. Incharoensakdi A, Waditee R. Degradation of glycinebetaine by betaine-homocysteine methyltransferase in *Aphanothece halophytica*: effect of salt downshock and starvation. Curr Microbiol. 2000;41:227-31.
60. Waditee R, Bhuiyan NH, Hirata E, Hibino T, Tanaka Y, Shikata M, et al. Metabolic engineering for betaine accumulation in microbes and plants. J Biol Chem. 2007;282:34185-93.
61. Waditee-Sirisattha R, Kageyama H, Fukaya M, Rai V, Takabe T. Nitrate and amino acid availability affects glycine betaine and mycosporine-2-glycine in response to changes of salinity in a halotolerant cyanobacterium *Aphanothece halophytica*. FEMS Microbiol Lett. 2015;362:fnv198.
62. Waditee R, Bhuiyan MNH, Rai V, Aoki K, Tanaka Y, Hibino T, et al. Genes for direct methylation of glycine provide high levels of glycinebetaine and abiotic-stress tolerance in *Synechococcus* and *Arabidopsis*. Proc Natl Acad Sci USA. 2005;102:1318-23.
63. He Y, He C, Li L, Liu Z, Yang A, Zhang J. Heterologous expression of *ApGSMT2* and *ApDMT2* genes from *Aphanothece halophytica* enhanced drought tolerance in transgenic tobacco. Mol Biol Rep. 2011;38:657-66.
64. Shkryl Y, Degtyarenko A, Grigorchuk V, Balabanova L, Tekutyeva L, editors. Betaine biosynthesis in a heterologous expression system based on the B12 producer *Pseudomonas denitrificans*. E3S Web of Conferences; 2020: EDP Sciences.
65. Kanesaki Y, Shiwa Y, Tajima N, Suzuki M, Watanabe S, Sato N, et al. Identification of substrain-specific mutations by massively parallel whole-genome resequencing of *Synechocystis* sp. PCC 6803. DNA Res. 2012;19:67-79.
66. Trautmann D, Voß B, Wilde A, Al-Babili S, Hess WR. Microevolution in cyanobacteria: re-sequencing a motile substrain of *Synechocystis* sp. PCC 6803. DNA Res. 2012;19:435-48.
67. Stanier R, Kunisawa R, Mandel M, Cohen-Bazire G. Purification and properties of unicellular blue-green algae (order *Chroococcales*). Bacteriol Rev. 1971;35:171-205.
68. Sambrook J, Russel D. Molecular Cloning: a laboratory manual. 3rd ed: Cold Spring Harbor Laboratory Press, NY, USA; 2001.
69. Tamagnini P, Troshina O, Oxelfelt F, Salema R, Lindblad P. Hydrogenases in *Nostoc* sp. strain PCC 73102, a strain lacking a bidirectional enzyme. Appl Environ Microbiol. 1997;63:1801-7.
70. Leitão E, Pereira S, Bondoso J, Ferreira D, Pinto F, Moradas-Ferreira P, et al. Genes involved in the maturation of hydrogenase(s) in the nonheterocystous cyanobacterium *Lyngbya majuscula* CCAP 1446/4. Int J Hydrog Energy. 2006;31:1469-77.
71. Silva-Rocha R, Martínez-García E, Calles B, Chavarría M, Arce-Rodríguez A, de las Heras A, et al. The Standard European Vector Architecture (SEVA): a coherent platform for the analysis and deployment of complex prokaryotic phenotypes. Nucleic Acids Res. 2013;41:D666-D75.

1012 72. Pinto F, Pacheco CC, Ferreira D, Moradas-Ferreira P, Tamagnini P. Selection of suitable
1013 reference genes for RT-qPCR analyses in cyanobacteria. PLoS One. 2012;7:e34983.
1014 73. Schafer A, Tauch A, Jager W, Kalinowski J, Thierbach G, Puhler A. Small mobilizable
1015 multi-purpose cloning vectors derived from the *Escherichia coli* plasmids pK18 and pK19:
1016 selection of defined deletions in the chromosome of *Corynebacterium glutamicum*. Gene.
1017 1994;145:69-73.
1018 74. Williams JG. Construction of specific mutations in photosystem II photosynthetic
1019 reaction center by genetic engineering methods in *Synechocystis* 6803. Methods Enzymol.
1020 1988;167:766-78.
1021 75. Meeks JC, Castenholz RW. Growth and photosynthesis in an extreme thermophile,
1022 *Synechococcus lividus* (Cyanophyta). Arch Microbiol. 1971;78:25-41.
1023 76. Mota R, Guimarães R, Büttel Z, Rossi F, Colica G, Silva CJ, et al. Production and
1024 characterization of extracellular carbohydrate polymer from *Cyanothece* sp. CCY 0110.
1025 Carbohydr Polym. 2013;92:1408-15.
1026 77. Dubois M, Gilles KA, Hamilton JK, Rebers PA, Smith F. Colorimetric method for
1027 determination of sugars and related substances. Anal Chem. 1956;28:350-6.
1028 78. Pereira SB, Santos M, Leite JP, Flores C, Eisfeld C, Büttel Z, et al. The role of the tyrosine
1029 kinase Wzc (Sll0923) and the phosphatase Wzb (Slr0328) in the production of extracellular
1030 polymeric substances (EPS) by *Synechocystis* PCC 6803. Microbiologyopen. 2019;8:e753.
1031 79. Ernst A, Kirschenlohr H, Diez J, Böger P. Glycogen content and nitrogenase activity in
1032 *Anabaena variabilis*. Arch Microbiol. 1984;140:120-5.
1033 80. Bustin SA, Benes V, Garson JA, Hellemans J, Huggett J, Kubista M, et al. The MIQE
1034 Guidelines: Minimum Information for Publication of Quantitative Real-Time PCR Experiments.
1035 Clin Chem. 2009;55:611-22.
1036 81. Santos H, Lamosa P, Borges N. Characterization and quantification of compatible solutes
1037 in (hyper)thermophilic microorganisms. In: Rainey FA, Oren A, editors. Extremophiles. 35:
1038 Methods in Microbiology, Academic Press; 2006. p. 173-99.
1039 82. Orth JD, Thiele I, Palsson BØ. What is flux balance analysis? Nat Biotechnol.
1040 2010;28:245-8.
1041

Supplementary Files

This is a list of supplementary files associated with this preprint. Click to download.

- Additionalfile1Fereiraetal.291021BiotechBiofuels.pdf
- Additionalfile2Ferreiraetal.291021BiotechBiofuels.pdf